

The background of the cover features a large, faint, circular seal of the University of Oslo. The seal contains a figure of a woman in classical attire playing a harp, surrounded by the Latin text 'UNIVERSITAS OSLOENSIS' and the date 'MDCCCXI' (1811).

U-Pb ID-TIMS geochronology and evolution of Caledonian Nappes in southern Norway

Cornelia Roffeis

Thesis submitted for the degree of Philosophiae Doctor

Faculty of Mathematics and Natural Sciences
Department of Geology

University of Oslo, September 2012

© Cornelia Roffeis, 2012

*Series of dissertations submitted to the
Faculty of Mathematics and Natural Sciences, University of Oslo
No. 1267*

ISSN 1501-7710

All rights reserved. No part of this publication may be
reproduced or transmitted, in any form or by any means, without permission.

Cover: Inger Sandved Anfinssen.
Printed in Norway: AIT Oslo AS.

Produced in co-operation with Akademika publishing.
The thesis is produced by Akademika publishing merely in connection with the
thesis defence. Kindly direct all inquiries regarding the thesis to the copyright
holder or the unit which grants the doctorate.



(The Upper Finse Nappe, Hardangervidda, Norway. Field season 2011)

'Geologists have a saying - rocks remember'
Neil Armstrong

Acknowledgement

Four years ago I arrived at the University of Oslo with the plan to write a PhD. In my luggage was a lot of ambition and determination but in fact I was not really aware of what doing a PhD actually meant and knew even less about how to succeed. But I was lucky, I got a lot of help and support along the way, and here and now, standing at the finish line, I want to express my gratitude to those people.

First and foremost I want to thank my main supervisor, Fernando Corfu, for his support, his help, his never ending patience in the lab or with correcting my papers, the good times in the field and for always having an open door for questions, discussions or just a chat. Fernando, you are an inspiration for every young scientist.

A big thank you also goes to my co-supervisors Arild Andresen and Roy Gabrielsen for advice and support whenever needed.

I want to thank Gunborg, Nana, and Magnus for support in the lab, Muriel and Berit for help with the microprobe and SEM, and Lars and Mattias for interesting and helpful discussions about zircons in general and the Caledonides in particular.

A big thank you goes to all my colleagues and friends at the Geology Department, who made my time at the institute unforgettable. Thank you Jacqueline, Derya, Deta, Andreas, Vincent, Tobi, Sebastian, Kirsten and all the others for the coffee chats, beer evenings, climbing and skiing adventures, and training sessions; thank you for the good times!

Last but not least, the biggest thank you goes 2000 km further south. Sabine, thank you for everything, I don't know what I would have done without you, our skype evenings and email conversations.

And finally, I want to thank my parents for their never-ending encouragement, support and the safe feeling that I can always rely on them.

Contents

Acknowledgement.....	1
Presentations at conferences	5
Preface	6
 INTRODUCTION.....	 9
1. Geochronology in the Caledonides	9
1.1. Why study the age of rocks?	9
2. The principles of Geochronology	10
2.1. Atomic structure	10
2.2. Isotopes	11
2.2.1. Radioactive decay.....	12
2.3. The application in geochronology	14
2.3.1. The choice of the right mineral	17
2.3.2. ID-TIMS.....	19
2.4. Zircon behavior in the nappes – What are we measuring?	20
2.4.1. Zircon textures and their implications	20
3. The formation of the Caledonides	22
3.1. Correlating the nappes.....	24
4. Introduction to the papers - questions, results and highlights	26
4.1. Paper #1	26
4.1.1. Facts and open questions:.....	26
4.1.2. Findings and conclusions:.....	26
4.2. Paper #2	28
4.2.1. Facts and open questions:.....	28
4.2.2. Findings and conclusions:.....	28
4.3. Paper #3	29
4.3.1. Facts and open questions:.....	29
4.3.2. Findings and conclusions:.....	29
4.4. Paper #4	31

4.4.1.	Facts and open questions:	31
4.4.2.	Findings and conclusions:	31
4.5.	General conclusions and outlook	32
	References.....	33

PAPER #1.....

Roffeis C, Corfu F, Austrheim H (2012) Evidence for a Caledonian amphibolite to eclogite facies pressure gradient in the Middle Allochthon Lindås Nappe, SW-Norway. Contribution to Mineralogy and Petrology 164:81-99 doi:10.1007/s00410-012-0727-7

PAPER #2.....

Roffeis C, Corfu F, Gabrielsen RH (in rev) A Sveconorwegian terrane boundary in the Caledonian Hardanger-Ryfylke Nappe Complex: the lost link between Telemarkia and the Western Gneiss Region? Accepted in Precambrian Research pending major revisions

PAPER #3.....

Roffeis C, Corfu F (in prep) Correlation of Caledonian crystalline nappes in SW-Norway by means of U-Pb geochronology: old problems and new data. Prepared for Special Publication of the Geological Society, London: 'New perspectives on the Caledonides of Scandinavia and related areas'

PAPER #4.....

Roffeis C, Corfu F (in prep) Evolution and origin of the Revsegg Nappe in the SW-Norwegian Caledonides: an allochthon with Ordovician elements. Prepared for Special Publication of the Geological Society, London: 'New perspectives on the Caledonides of Scandinavia and related areas'

Presentations at conferences

AGU Spring meeting 2009, Toronto

Poster: Deformation and recrystallization of zircon and its influence on the isotope systems: a case from a shear zone in anorthosite of the Lindås nappe.

Roffeis C, Austrheim H, Piazzolo S, Corfu F, Simonsen S

Nordic Geological Winter Meeting 2010, Oslo

Poster: Links between breakdown of garnet, zircon deformation and resetting of the U-Pb systems: a case from the Lindås Nappe, SW Norway.

Roffeis C, Austrheim H, Piazzolo S, Corfu F, Simonsen S

EGU General Assembly 2010, Vienna

Talk: The influence of deformation on zircon and the effect on their isotope system: a case study from the polymetamorphic Lindås Nappe, SW-Norway.

Roffeis C, Corfu F, Austrheim H, Piazzolo S

Goldschmidt Conference 2011, Prague

Poster: ID-TIMS as a tool for terrane provenance studies in polyorogenic complexes: a case from the SW-Norwegian Caledonides.

Roffeis C, Corfu F, Gabrielsen RH

EGU General Assembly 2012, Vienna

Poster: A slice of Upper Allochthon in a Middle Allochthon terrain? An ID-TIMS U-Pb study of the Hardanger-Ryfylke Nappe Complex, SW-Norway.

Roffeis C, Corfu F, Gabrielsen RH

Goldschmidt Conference 2012, Montreal

Poster: Discordant polymetamorphic zircons: the rule in crystalline nappes of the SW Norwegian Caledonides.

Roffeis C, Corfu F

Preface

This work is placed in the Caledonides, the mountain range stretching from north to south all along the west coast of Norway and reaching further inland in the southern part. It consists of allochthonous nappes, thrust on autochthonous basement rocks during the Caledonian orogeny. The goal of this thesis is the collection of age data for establishing detailed geochronological profiles for various nappes in the SW-Norwegian Caledonides. Based on these, comparison, classification, and distinction of the nappes in terms of their provenance, evolution and the role they played in the Caledonian orogeny are discussed.

For geologists, the Caledonides are an intriguing working place, since they provide an excellent natural observatory for mountain building processes. Once being a mighty mountain range comparable to the present day Himalayas, erosion during the last 430 Ma exposed the “inner” part of the orogen and allows geologists to study processes, which partly occurred deep in the crust. Furthermore, the nappes provide more than just information about this latest orogenic event; being mainly thrust parts of the Baltic continent, they contain valuable information about the pre-Caledonian history of Baltica: the formation of the Baltic crust and the Sveconorwegian orogeny.

Rocks in the Caledonides show a great variety of lithologies which can, despite thorough mapping and structural analysis, make it difficult to differentiate between the various nappes and even more difficult to group those with similar evolution and origin together. That is where geochronology becomes an important tool: by determination of the protolith age and the timing of metamorphic overprints, co-genetic parts can be identified and furthermore tentatively assigned to autochthonous rocks which might have served as provenance areas for the Caledonian thrusting. The Caledonian orogeny can then be rewound, which leads to a better understanding of the thrusting and orogenic processes, and it allows us to analyze the pre-Caledonian evolution of the area.

This thesis provides new geochronological data for several different nappes, compares and combines them with existing data sets and finally incorporates the new information into an interpretation of the systematics in the SW-Norwegian Caledonides. It thereby contributes to a better understanding of the Caledonian as well as of the Sveconorwegian evolution.

Four papers have been written, each concentrating on different nappes and tackling the specific problems of the individual areas. The used method was ID-TIMS U-Pb geochronology, mainly on zircon. The following introduction will therefore first explain the principles of geochronology with emphasis and description of the used method and, second, provide a geological background for the Caledonides in Norway, containing an introduction on zircon behavior in such polyorogenic terrains. The papers are found after the introduction in chronological order of development. A short summary of the main findings and conclusions is given at the end of the introduction. Cross references in the introduction to the papers are given with the paper numbers, #1 to #4.

1. Geochronology in the Caledonides

1.1. Why study the age of rocks?

One might say developments in geochronology were driven by pure curiosity. It started with the desire to know how old our planet is. Throughout history many scientists, at the beginning mainly physicists, tried variable approaches to determine the age of the Earth with even more varying results; Lord Kelvin calculated an age of the Solar system based on gravitational collapse energy, John Jolly estimated an age of the Earth by the assumption of salts in the ocean being brought in by rivers with constant rates, just to name two of the main players in the science community in the late 19th century. The determined ages ranged from 100 Ma to 20 Ma and did not satisfy the geological community, but finally with the discovery of radioactivity by Henri Becquerel in 1896 a new tool was at hand. Not more than 11 years later Bertram Boltwood published the first 'radiometric age'; he measures the Pb concentration in pitchblende. But it took until the mid 20th century before Alfred Nier started using isotopic ratios rather than element abundance. Mass spectrometers evolved from Niers design from 1940 and started to appear in more and more geological laboratories (White, in print). Modern geochronology was born.

And it still improves. Laboratory procedures evolve, so do machines, standards were introduced, decay constants refined, and the precision of age calculation keeps improving. But why is it so important to get even more accurate ages of rocks? This is best answered by using this thesis: With all the findings and achievements in geochronology, we now have the tools not just to date the age of formation of rocks, but also later processes, such as metamorphic overprints, retrogression, deformation, fluid activity, to name the most common ones. We can determine rates and pathways of geological evolution. And the Caledonides provide an excellent study area for that. Formed during a collisional event 430 Ma ago, the history of the rocks involved is much older; also many different lithologies occur with different reactions to certain events. Data from this area gives an insight into the variety and timing of processes involved in repeated mountain building processes.

2. The principles of geochronology

The principle of being able to date geological events is the accumulation of unstable parent isotopes in a specific mineral during crystallization. The parent isotopes gradually decay and the daughter isotopes accumulate in the same crystal. The amounts and ratios of the isotopes can be measured, and with the known decay constants, the age since the formation of the crystal can be calculated. The following chapters will give a short summary of the principles of isotope geology, and describe in more detail the method used in this thesis, U-Pb ID-TIMS geochronology.

2.1. Atomic structure

The essential components of an atom can be described with a small, positively charged nucleus containing most of the atoms' mass, and a surrounding cloud of electrons with a negative charge. The nucleus is only about 10^{-12} cm in diameter, but contains a number of elementary particles, referred to as nucleons. For the purpose of this introduction, only protons and neutrons, being mostly responsible for the weight and the charge of the nucleus, are discussed. The number of negatively charged electrons in the cloud equals the number of positively charged protons in the nucleus. Neutrons have no charge, and are equal or higher in number than protons with one exception being ^1H (Hydrogen) which has one proton and no neutron.

The number of protons, which in turn also predict the number of electrons, defines the chemical behavior of an atom and thus provides the basis for notation of elements in the periodic table (Fig. 1), where the main numbers are the mass number (A), the number of protons (Z) and the number of neutrons (N), which relate as: $A=Z+N$

The classification of elements in the periodic table follows the number of protons (Z), the atomic number, in ascending order. A common notation outside the periodic table gives the chemical symbol and two numbers to the left, one in superscript, one in subscript, e.g. ^4_2He where 4 is the total number of nucleons (A) and 2 is the number of protons (Z), also indicating that He is found at the 2nd place in the atomic table (Faure and Mensing 2005).

hydrogen

1

H

1.00784

lithium

3

Li

6.941

sodium

11

Na

22.98977

potassium

19

K

39.0983

rubidium

37

Rb

85.4678

cesium

55

Cs

132.90545

francium

87

Fr

[223]

beryllium

4

Be

9.012182

magnesium

12

Mg

24.3050

calcium

20

Ca

40.078

strontium

38

Sr

87.62

barium

56

Ba

137.327

radium

88

Ra

[226]

scandium

21

Sc

44.95591

titanium

22

Ti

47.867

vanadium

23

V

50.9415

chromium

24

Cr

51.9961

manganese

25

Mn

54.93805

iron

26

Fe

55.845

cobalt

27

Co

58.9332

nickel

28

Ni

58.6934

copper

29

Cu

63.546

zinc

30

Zn

65.409

gallium

31

Ga

69.723

germanium

32

Ge

72.64

arsenic

33

As

74.9216

selenium

34

Se

78.96

bromine

35

Br

79.904

krypton

36

Kr

83.798

yttrium

39

Y

88.90585

zirconium

40

Zr

91.224

niobium

41

Nb

92.90638

molybdenum

42

Mo

95.94

technetium

43

Tc

[98]

ruthenium

44

Ru

101.07

rhodium

45

Rh

102.9055

palladium

46

Pd

106.42

silver

47

Ag

107.8682

cadmium

48

Cd

112.411

indium

49

In

114.818

tin

50

Sn

118.710

antimony

51

Sb

121.760

tellurium

52

Te

127.60

iodine

53

I

126.9045

xenon

54

Xe

131.293

lanthanum

57

La

138.9055

cerium

58

Ce

140.116

praseodymium

59

Pr

140.90765

neodymium

60

Nd

144.24

promethium

61

Pm

[145]

samarium

62

Sm

150.36

europium

63

Eu

151.964

gadolinium

64

Gd

157.25

terbium

65

Tb

158.9253

dysprosium

66

Dy

162.50

holmium

67

Ho

164.930

erbium

68

Er

167.259

thulium

69

Tm

168.934

ytterbium

70

Yb

173.04

actinium

89

Ac

[227]

thorium

90

Th

232.038

protactinium

91

Pa

231.0369

uranium

92

U

238.0289

neptunium

93

Np

[237]

plutonium

94

Pu

[244]

americium

95

Am

[243]

curium

96

Cm

[247]

berkelium

97

Bk

[247]

californium

98

Cf

[251]

einsteinium

99

Es

[252]

fermium

100

Fm

[257]

mendelevium

101

Md

[268]

nobelium

102

No

[259]

Element name

Atomic number (Z)

Element symbol

Atomic mass

hydrogen

1

H

1.00784

lithium

3

Li

6.941

sodium

11

Na

22.98977

potassium

19

K

39.0983

rubidium

37

Rb

85.4678

cesium

55

Cs

132.90545

francium

87

Fr

[223]

beryllium

4

Be

9.012182

magnesium

12

Mg

24.3050

calcium

20

Ca

40.078

strontium

38

Sr

87.62

barium

56

Ba

137.327

radium

88

Ra

[226]

scandium

21

Sc

44.95591

titanium

22

Ti

47.867

vanadium

23

V

50.9415

chromium

24

Cr

51.9961

manganese

25

Mn

54.93805

iron

26

Fe

55.845

cobalt

27

Co

58.9332

nickel

28

Ni

58.6934

copper

29

Cu

63.546

zinc

30

Zn

65.409

gallium

31

Ga

69.723

germanium

32

Ge

72.64

arsenic

33

As

74.9216

selenium

34

Se

78.96

bromine

35

Br

79.904

krypton

36

Kr

83.798

yttrium

39

Y

88.90585

zirconium

40

Zr

91.224

niobium

41

Nb

92.90638

molybdenum

42

Mo

95.94

technetium

43

Tc

[98]

ruthenium

44

Ru

101.07

rhodium

45

Rh

102.9055

palladium

46

Pd

106.42

silver

47

Ag

107.8682

cadmium

48

Cd

112.411

indium

49

In

114.818

tin

50

Sn

118.710

antimony

51

Sb

121.760

tellurium

52

Te

127.60

iodine

53

I

126.9045

xenon

54

Xe

131.293

lanthanum

57

La

138.9055

cerium

58

Ce

140.116

praseodymium

59

Pr

140.90765

neodymium

60

Nd

144.24

promethium

61

Pm

[145]

samarium

62

Sm

150.36

europium

63

Eu

151.964

gadolinium

64

Gd

157.25

terbium

65

Tb

158.9253

dysprosium

66

Dy

162.50

holmium

67

Ho

164.930

erbium

68

Er

167.259

thulium

69

Tm

168.934

ytterbium

70

Yb

173.04

actinium

89

Ac

[227]

thorium

90

Th

232.038

protactinium

91

Pa

231.0369

uranium

92

U

238.0289

neptunium

93

Np

[237]

plutonium

94

Pu

[244]

americium

95

Am

[243]

curium

96

Cm

[247]

berkelium

97

Bk

[247]

californium

98

Cf

[251]

einsteinium

99

Es

[252]

fermium

100

Fm

[257]

mendelevium

101

Md

[268]

nobelium

102

No

[259]

Element name

Atomic number (Z)

Element symbol

Atomic mass

Fig. 1 Periodic table of elements (modified after http://www.bpc.edu/mathscience/chemistry/history_of_the_periodic_table.html). The entries are explained by the example of calcium. U, Th and Pb, the most important elements for this study, are framed.

2.2. Isotopes

In the example of the ^4He -isotope, the number of neutron (N), given by (A)-(Z), is 2 and equivalent to the number of protons. However, most of the elements have several isotopes, i.e. nuclei with a different number of neutrons. The average number of nucleons, i.e. the atomic mass (Fig. 1), is generally larger than twice the proton number.

How many more neutrons than protons a core can incorporate, meaning how many different isotopes of one specific element exist, depends on the element itself. However, when the (N)/(Z) ratio in an isotope is getting too high, it becomes unstable and decays to stable so-called “daughter” isotopes. One can therefore distinguish between stable and unstable isotopes. Unstable isotopes and their predictable decay to stable isotopes are the basis of geochronology.

Age calculation is done on ratios between parent and daughter isotopes. In this study the Uranium (U) – Thorium (Th) – Lead (Pb) isotope system is used and will therefore be explained in more detail in the following.

The best way to display isotopes is with the chart of nuclides, where (N) on the x-axis is plotted against (Z) on the y-axis and therefore isotopes of one element are noted in

one row (Fig. 2). Vertical rows are called isotones and contain different elements, but with the same number of neutrons. Isotopes of different elements with the same (A) are called isobars (Faure and Mensing 2005).

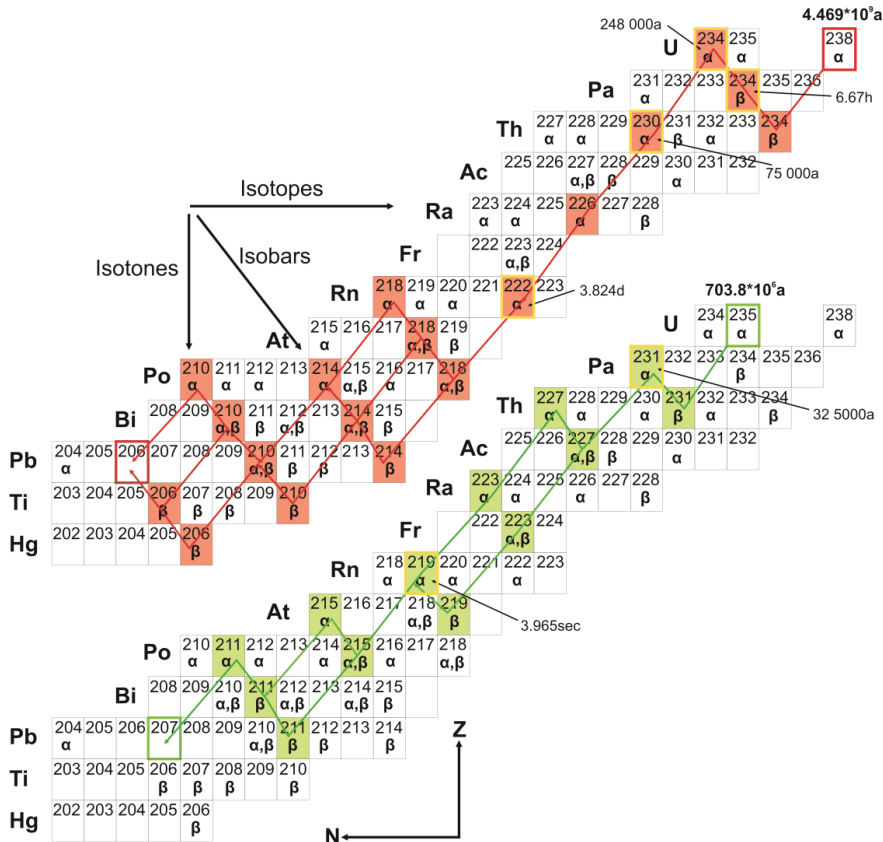


Fig. 2 Chart of nuclides (modified after White, in print). The decay series of ^{235}U and ^{238}U are displayed. The exact decay path can be seen following the arrows. α -decay is the loss of two protons and two neutrons, β -decay means the loss of an electron. The intermediate products of the decay series are colored, those where the excess or loss of the element in certain minerals might alter the amount of the daughter isotope, are framed.

2.2.1. Radioactive decay

Unstable isotopes decay to stable daughter isotopes, possibly forming unstable intermediate product isotopes along the way (Fig. 2). Decay rates are constant over time and independent of external factors such as temperature or pressure. The rate is only dependent on the nature of the nuclide. It is commonly given by the half-life which is the

time elapsed until half of the parent isotope has decayed. Different decay mechanisms are known:

- α decay: the parent isotope is emitting a particle with two protons and two neutrons (a He nucleus).
- β decay: the parent isotope is emitting an electron or positron. A neutron converts to a proton or vice versa; thereby the charge of the nucleus changes, but not the number of nucleons.
- γ decay: radiation (a high energy photon) is emitted. It can accompany other decays to balance out the energy level.
- electron capture: emission of a neutrino from the nucleus and capture of an electron, a proton converts to a neutron.
- spontaneous fission: occurs only in the heaviest nuclei, such as ^{238}U , and is rare. The nucleus splits into two still heavy daughter nuclei, which are most likely unstable themselves.

The geochronological work performed in this thesis is based on the decay of the long lived isotopes of U (and Th) to Pb. The decay path over intermediate products is defined by α - and β -decay mechanism. U forms three isotopes: ^{234}U , ^{235}U and ^{238}U , however ^{234}U is an intermediate product of the ^{238}U decay series. The main decay series are therefore ^{235}U , decaying to ^{207}Pb (half-life = 703.8 m.y.), and ^{238}U decaying to ^{206}Pb (half-life = 4469 m.y.). The U to Pb decay provides a special case in geochronology since with the different isotopes of the same elements one can rely on two systems for getting one age; a powerful tool.

Thorium concentration is commonly not measured, because in most minerals used for geochronology, e.g. zircon and titanite, Th is by far less abundant compared to U. However, an abundance is usually determined with the ^{208}Pb isotope, deriving from the decay of ^{232}Th (half-life = 14000 m.y.), to get an idea about the Th/U ratio in the mineral. Thorium isotopes (except ^{232}Th) are however intermediate, short lived products (in geological timescale) in the U decay series. Chemical fractionation events can cause isotopic disequilibrium of a decay series. Intermediate decay products which are prone for excess or loss are marked with a yellow frame in Fig. 2. Thorium is one of those. Excess Th, for example, in monazite, a mineral with a higher tendency to incorporate Th, can lead to excess of ^{206}Pb , deriving from ^{230}Th . Another example for a potential disequilibrium is ^{222}Rn ,

an intermediate product of the ^{238}U decay series, which is a gas and can therefore escape from the system, for example during weathering. Another element to consider is ^{231}Pa , which is an intermediate product in the ^{235}U chain (Faure and Mensing 2005; White, in print).

2.2.1.1. *Calculating decay*

The decay of an unstable isotope over time can be expressed by the simple equation:

$$dN/dt = -\lambda N$$

where dN is the change of the amount of atoms of the parent isotope, dt is the change in time and λ is the decay constant, a value specific to the isotope in question. The minus indicates the decrease of material. Integrating this equation over time and resolving with the half-life of an isotope leads to the general equation of decay:

$$D = D_0 + N(e^{\lambda t} - 1)$$

where D is the amount of the daughter isotopes (D_0 plus what is deriving from the decaying parent isotopes). D_0 is the same isotope already present before the decay started (which might be 0 in some minerals, discussed later), N is the parent isotope and λ is the decay constant. This equation can now be resolved for t (time):

$$t = \frac{1}{\lambda} \ln\left(\frac{D - D_0}{N} + 1\right)$$

In this general term we could now fill in for example ^{206}Pb and ^{238}U for D and N and determine the time it took to form the Pb from the U. The equation, however, is just the basis. In geochronology, not the absolute abundances of isotopes, but ratios are measured since it is easier and can be done with higher accuracy. The principal equation using ratios of isotopes is however essentially the same:

$$R = R_0 + R_{P/D}(e^{\lambda t} - 1)$$

where R_0 is the initial ratio and $R_{P/D}$ is the parent/daughter ratio. To obtain a good date, several ratios and derivatives of the general equation are used (White, in print).

2.3. The application in geochronology

Radioactive decay is independent of external factors such as temperature and pressure as well as of the previous history of the isotope. The radioactive clock starts ticking

when the parent isotope is embedded in the crystalline structure of a mineral. After the mineral's formation the radioactive parent isotopes decay, forming daughter isotopes, which commonly stay in the same crystal as the parent.

Minerals have preferences for incorporation specific elements, and later processes in the crust affect different minerals in different ways. The key element for geochronology is therefore to choose the system and mineral fitting best to the geological questions of an area. This thesis works with the U-(Th)-Pb system. In general one can say, longer half-lives allow to date older events. The U and Th isotopes have long half-lives and can therefore date the oldest events in Earth history down to the formation of the first crust. It is the perfect system for the long and old history of the Caledonides. However, the abundance of U and Th is low. Since large ions are incompatible in early crystallizing minerals during crystallization of magma, they are concentrated in the liquid phase, and incorporated into minerals crystallizing last, hence mainly occur in silica rich rocks forming the continental crust. Progressive geochemical differentiation of the upper mantle has enriched the continental crust in U (2.7 µg/g) and Th (10.5 µg/g) (Winter 2001; Rudnick and Gao 2003). However, they are mostly restricted to specific minerals with suitable crystallographic sites. Both elements are large, have similar radii, a 4+ oxidation state and can therefore substitute each other and other elements with comparable properties like e.g. Zr in zircon. The amount of U, Th and the U and Th ratios not only provide a basis for the age, but also gives information about the crystallization conditions and environment of a sample. For instance felsic late magmatic melts tend to incorporate more U than mafic ones. The main factor that can affect the Th/U ratio is the solubility of the uranyl ion (UO_2^{2+}) in water formed under oxidizing conditions. The U in this form is mobile and can be separated from the Th (Faure and Mensing 2005).

Once the minerals incorporating U and Th crystallized, the decay is underway. ^{235}U decays faster than ^{238}U . In a diagram with both of these decay series plotted against each other, undisturbed decay from U to Pb forms a curve which represents a time line, and is called Concordia. The diagram is hence a Concordia diagram (Fig. 3). $^{206}\text{Pb}/^{238}\text{U}$ plots on the y-axis, $^{207}\text{Pb}/^{235}\text{U}$ on the x-axis. Every point on Concordia is an age, provided that no Pb or U has escaped or been added to the system. However, Pb is a more mobile element than U and could escape a mineral during geological events, which makes Pb loss a common feature of metamorphism. Since Pb isotopes do not fractionate, also Pb depleted samples follow a system in the way they plot on a Concordia diagram. They fall off the curve –

getting discordant – and plot along a line between their original age and the event causing the Pb loss, which are given by the intercepts of the line with Concordia. The more Pb they lose, the more discordant they get (Faure and Mensing 2005). Discordant data points can also be the result of mixing of different zircon generations, e.g. an older core and a younger rim, formed during a later event, in one zircon grain. An example is given in Fig. 3, which stems from a sample from paper #2. Single minerals or mineral fractions provide data points with error ellipses on the Concordia diagram. The data points are discordant, indicating most likely Pb loss during metamorphism. A discordia line intersects Concordia at 1627 ± 61 and 989 ± 91 Ma. The older age is considered the age of formation of the minerals, the time when the U started to decay. The younger age gives the event that caused the disturbance in the isotope ratios. This example is of course a simple case. Often several events occur and overlap within the data which can cause a scatter of data points (see discussions in paper #1 - #4).

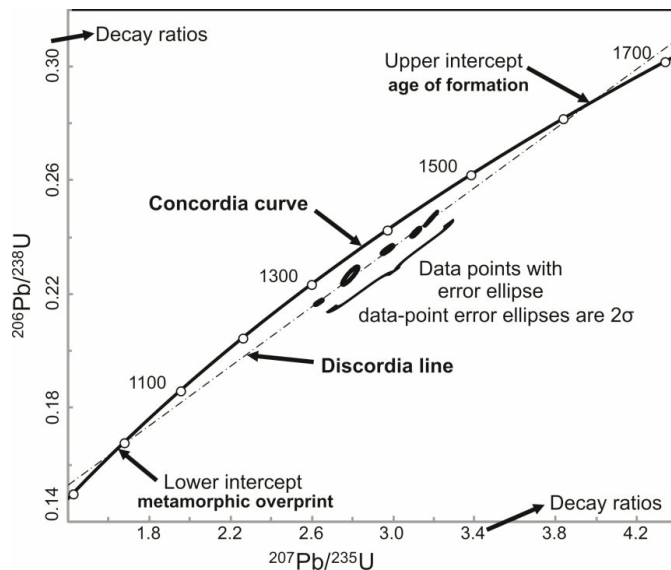


Fig. 3 Example of a Concordia diagram with discordant samples, forming a discordia line. The data stems from a gneiss in the Kvitenut Nappe, presented in paper #2.

2.3.1. The choice of the right mineral

The crystallization of a mineral (the mineral's specific closing temperature) is considered the starting point of the radioactive clock. This is the age obtained by dating if nothing disturbs the isotopes later. Disturbance in the U–Pb isotope system heavily depends on the mineral and its reaction to geological events. A key element in dating rocks is therefore the choice of minerals. A good dating mineral should incorporate a high amount of U and should ideally keep out, or at least minimize, Pb from the initial crystal ($D_0=0$). This way it can be assured that the Pb in the mineral only derives from decay and no common Pb correction has to be performed. If that is not the case the isotopic composition for D_0 has to be measured or modeled. The ideal mineral should also occur in a great variety of rocks (Faure and Mensing 2005). The minerals used for this thesis are mainly zircon, but also titanite, rutile, monazite and apatite. These minerals are formed by and react differently to geological events and hence date different things. This study only uses magmatic or metamorphic samples and the minerals are discussed in respect to that. A short summary of each is given in the following:

2.3.1.1. Zircon ($ZrSiO_4$)

Zircon is the most important mineral in geochronology and also the one used most in this thesis. It is an accessory mineral that occurs in most of the crustal rocks, but it is sparse in mafic rocks such as gabbros or anorthosites (paper #1). In many ways zircons are ideal for geochronology; they can easily incorporate U in the mineral structure, but reject Pb, which means that zircons are normally clean in terms of common Pb. Moreover, they are robust. Closing temperature is $> 900^\circ\text{C}$ for Pb diffusion (Cherniak and Watson 2001), which means zircons date the crystallization event, and are normally not easily reset by later events. Therefore, they can contain the oldest ages of rocks, and date the formation of crust. However, one cannot a priori assume that zircons always give the oldest age of a sample because they can also form during metamorphism, metasomatic events or in partial melts (e.g. paper #1). Due to their high closing temperatures zircons should in theory sustain most geological events, however, Pb loss, resulting in discordant data, is very common. Lead might escape the crystal lattice when parts of the crystal are re-crystallized due to deformation (paper #1), or when the crystal is damaged because of the decay. The latter case (radiation damage) is called metamictisation and primarily occurs in minerals

high in U. The lattice is destroyed by escaping α –particles and recoil energy. The damage manifests itself in a brown color (Faure and Mensing 2005).

In many cases, especially in polymetamorphic terrains like the Caledonides, more than one generation of zircon can occur in one sample. Careful distinction of different zircon generations can reveal several events.

2.3.1.2. Titanite CaTiSiO_5

Titanite can incorporate U, but typically also contains common Pb, which requires a correction either with modeled values (Stacey and Kramers 1975) or by measuring a co-genetic phase, for example plagioclase, which only contains common Pb and no radiogenic Pb, for determining the isotope ratio of common Pb at the time of crystallization. Titanite can reveal original ages, but its closing temperature of Pb diffusion is ca 660 - 700°C (Scott and St-Onge 1995), therefore it might also date cooling. In addition it can form during a metamorphic event. Titanite in a sample, especially together with zircon data, can be helpful in revealing multiple growing events and metamorphic overprints (e.g. Tucker et al. 2004; paper #2; paper #3).

2.3.1.3. Rutile TiO_2

Rutile often occurs in mafic rocks where zircons and titanites are sparse. However, rutile can form magmatically, but also metamorphically, and it is usually not obvious to assign the grains to one or the other genesis. Also the dark color prevents from seeing through them, so inclusions can never be excluded. Common Pb is an issue, especially when inclusions can be present. Closing temperature of Pb diffusion in rutile is about 600°C (Cherniak 2000), allowing rutile to date cooling events in some cases if the peak metamorphic conditions were higher. Careful interpretation of equilibrium parageneses is therefore important. Rutile is often found as a core in titanite (e.g. paper #4).

2.3.1.4. Monazite $\text{LREE}(\text{PO}_4)$

Monazite has a high closing temperature (Cherniak et al. 2004) which makes it suitable to preserve the magmatic history, but it also has a wide stability field, which allows it to grow during metamorphism, in most cases above greenschist facies (Spear and Pyle 2002). It commonly incorporates high amounts of U, also of Th, is low in common Pb and not easily reset, so it commonly gives concordant data. However, its tendency to

incorporate a lot of Th can lead to excess ^{206}Pb from ^{230}Th . Monazite is a common mineral in metapelitic rocks and as such can be useful to date metamorphic events.

2.3.1.5. *Apatite $\text{Ca}_5(\text{PO}_4)_3(\text{F,Cl,OH})$*

Apatite can be used for ID-TIMS, which has been done in this thesis in paper #4. However, analyzing can be difficult because apatite is typically low in U, but incorporates common Pb. It commonly reveals metamorphic ages (Cherniak et al. 1991).

2.3.2. ID-TIMS

Isotope dilution thermal ionization mass spectrometry (ID-TIMS) is the method used in this thesis. It is the most accurate tool for dating, but it requires a lot of laboratory work. The specific laboratory procedures are described in the papers and only mentioned in short here: representative samples are taken from the field and crushed, minerals are separated by magnetic separation and heavy liquid, and then zircons (or other minerals, depending on the question at hand) are hand picked. Mainly single grains were used, in order to avoid mixing ages from the polymetamorphic area. Air or chemical abrasion is performed on all zircons, in addition some titanites have been subjected to air abrasion. After spiking, dissolving the minerals, chemical separation, and loading, the samples were measured in a mass spectrometer. Isotope dilution, where the sample is mixed with a spike with known concentration of isotopes, provides a great accuracy for measuring isotopic ratios. Measurements can be performed on samples with less than $1\text{ }\mu\text{g}$, or grains with only 3 ppm U (e.g. paper #1).

The principle of a mass spectrometer is to separate charged atoms and molecules on basis of their masses when they move through a magnetic field. Modern mass spectrometers consist of a source of a monoenergetic beam of ions, a magnetic analyzer and an ion collector. For analyzing samples, a salt of the element is loaded on a filament and mounted in the source. The filament is then heated up to volatilize the elements, and the heat of the filament causes ionization of the atoms in the vapor. The ions are then accelerated into a beam. The beam enters the magnetic field which is perpendicular to the travel direction of the ions. The ions are deflected into curved paths where the radii are proportional to their masses. The separated ion beams continue through the analyzer to the collector where they generate a positive electrical charge. The ion beam is focused

through a collector slit and enters the detector cup, specific for one isotope. The beam that enters the cup is neutralized by electrons that flow through a resistor. The voltage difference is amplified and measured. Multiple collectors can measure several beams simultaneously. The signal consists of a series of peaks, each representing a mass to charge ratio, specific to one isotope. The height of the peak is proportional to the abundance of the isotope (Faure and Mensing 2005).

2.4. Zircon behavior in the nappes – What are we measuring?

The most important question when acquiring age data is: what are we actually measuring? As a first confinement, only U-Pb ages are dealt with in this thesis, but also the minerals chosen for dating play an important role in what process will be dated. Even when using only one mineral, different generations of this mineral can still occur in one sample. Since zircon is the mineral mostly used in this thesis, some more details about zircon behavior and implication for age dating are given in the following. The zircon population in a sample – especially in polymetamorphic terranes as dealt with here – can be quite manifold. Zircons with different shapes and colors, possible inclusions, degree of rounding or of metamictisation, can occur and indicate different generations (Corfu et al. 2003). Assigning the various zircon grains, and/or different zircon domains in one and the same grain, to specific events and to analyze them separately, are the key elements to determine a rock's entire history. In this study mainly single grains were used. This has the advantage to minimize mixing of zircons from different generations.

2.4.1. Zircon textures and their implications

In general, zircon is considered to be chemically robust under the range of conditions presented in the Earth's crust (Faure and Mensing 2005). That means zircons normally preserve the original age of formation. However, that does not mean that they remain completely unaffected by later events like metamorphism and deformation as e.g. demonstrated with discordia lines (Fig. 3).

Zircon has a tetragonal crystal shape and normally grows as doubly terminated prismatic crystal with elongation ratios between 1 and 5 (Corfu et al. 2003). Some general

features are observed: euhedral grains are commonly formed during the magmatic event, subrounding indicates a metamorphic overprint. Grains with “flat” tips, meaning [101] interfaces combined with [110] prisms, are commonly related to hydrous magmas such as pegmatites. These grains are also often metamict. Zircon forming events and partial alteration can alter or add to an existing grain.

Often a zircon preserves the original growth pattern in the core, but re-crystallizes at the rim. Subrounding or new overgrowths are also common. In addition, new zircons in an older sample can form during metamorphism. The challenge is to differentiate the single events and date them separately. CL images reveal the internal structure of a zircon, but most of the time the important features can also be seen under a binocular. Deciding, which grain to use for analysis is essential for the interpretation of the resulting age. For example, a core can reveal the crystallization age, and a rim can give the metamorphic overprint. For ID-TIMS analysis the chosen zircon grains have to have formed during one event only – magmatic or metamorphic - or a mixed (discordant) age will be the result. A core can be separated from a rim by abrasion. Analyzed separately, two stages in a rocks history can be dated.

The observation that zircons in high-grade metamorphic rocks retain their age of formation and preserve compositional growth zonation, assumes slow diffusion rates, even at high temperatures (Connelly 2001). The slow diffusion rate for Pb furthermore indicates that Pb isotope ratios will not be altered by volume diffusion under most geological conditions. Therefore element mobility in zircon, most importantly Pb-loss, is related to re-crystallization, hydrothermal activity and weathering or Pb transport in zircons with severe radiation damage (metamictization due to high U) (Cherniak and Watson 2001). A recent discussion also concerns the role of crystal-plastic deformation and microstructures (e.g. dislocations, low-angle orientation boundaries and sub grains) in zircon and their effect on zircon geochemistry (Reddy et al. 2006).

The mentioned observations on zircon shapes and their implications are general and might not be true for every sample. Throughout the four papers, some special cases have been dealt with. For example in paper #1 a case of deformed, low-U zircons suffering Pb loss is discussed. Paper #2 and #3 deal, among other things, with partly re-crystallized zircons with specific discordance pattern, and paper #4 describes some samples with magmatic, metamorphic, and inherited zircons.

3. The formation of the Caledonides

The Caledonides were once a large mountain range, formed during the Caledonian orogeny, when Baltica and Laurentia collided after the closure of the intervening Iapetus Ocean (Stephens and Gee 1985; Torsvik et al. 1996). However, the geological history of SW-Norway includes an older pre-history. The basement rocks of Baltica consist of crust of Mesoproterozoic age, which was extensively reworked already during the Sveconorwegian orogeny (ca 1140 to 900 Ma). The age of crust formation and the expressions of the Sveconorwegian event can be used to subdivide the basement into several terranes (Bingen et al. 2008a; Bingen et al. 2008b; Bingen et al. 2005). The Scandian phase (430-400 Ma) of the Caledonian orogeny (ca 480 to 400 Ma) led to southeast directed thrusting of nappes containing rocks derived from both continents, Baltica and Laurentia as well as from the Iapetus Ocean, onto Baltica. This series of nappes, emplaced on the Baltican Precambrian basement with its Cambro-Silurian autochthonous/paraautochthonous cover, form the Caledonian mountain belt. The collision also led to extreme crustal thickening when the leading edge of Baltica was subducted, extensively deformed and exposed to HP/UHP metamorphic conditions (Andersen and Andresen 1994; Fossen 2000; Kylander-Clark et al. 2009). The orogen was subsequently modified by extension and erosion (e.g. Andersen and Jamtveit 1990; Fossen 1998). Today the Caledonides are represented by a series of allochthonous nappes, partly laterally disconnected, lying on Baltic basement.

Some of the nappes have been transported for hundreds of kilometers whereby the uppermost nappes experienced the longest transport. According to their origin the nappe pile has traditionally been divided into 4 units: The Lower Allochthon represents detached slices of Baltican basement and overlying sediments. The Middle Allochthon is also inferred to be of Baltican origin, but these mainly crystalline nappes had a longer transport and probably derived from the destroyed deeper margin of Baltica. The Upper Allochthon derives from the outermost margin of Baltica and contains remnants of the Iapetus Ocean, and the Uppermost Allochthon comprises rocks of Laurentian affinity (Ramberg et al. 2008; Roberts 2003). That subdivision of the allochthons is the basis of the tectonostratigraphic map of Norway (Gee et al. 1985). The distinction, however, is crude and applied to the scale of the whole Caledonides, it often fails to explain regional details. In the study area of SW-Norway many inconsistencies occur. In that area, the dominant Caledonian nappes are assigned to the Middle Allochthon, containing mainly crystalline rocks, in most cases

underlain by Lower Allochthon, which mainly comprises phyllites. The largest of these Middle Allochthonous nappes is the Jotun Nappe Complex, surrounded by smaller nappes and nappe complexes, namely the Lindås-, Dalsfjord-, Espedalen-, Finse- and Hallingskarvet nappes and the Hardanger-Ryfylke Nappe Complex (HRNC) (Fig. 4). The affiliation with the Middle Allochthon implies a Baltican provenance of the nappes and therefore a shared evolution with the autochthonous basement terranes (Gee et al. 1985).

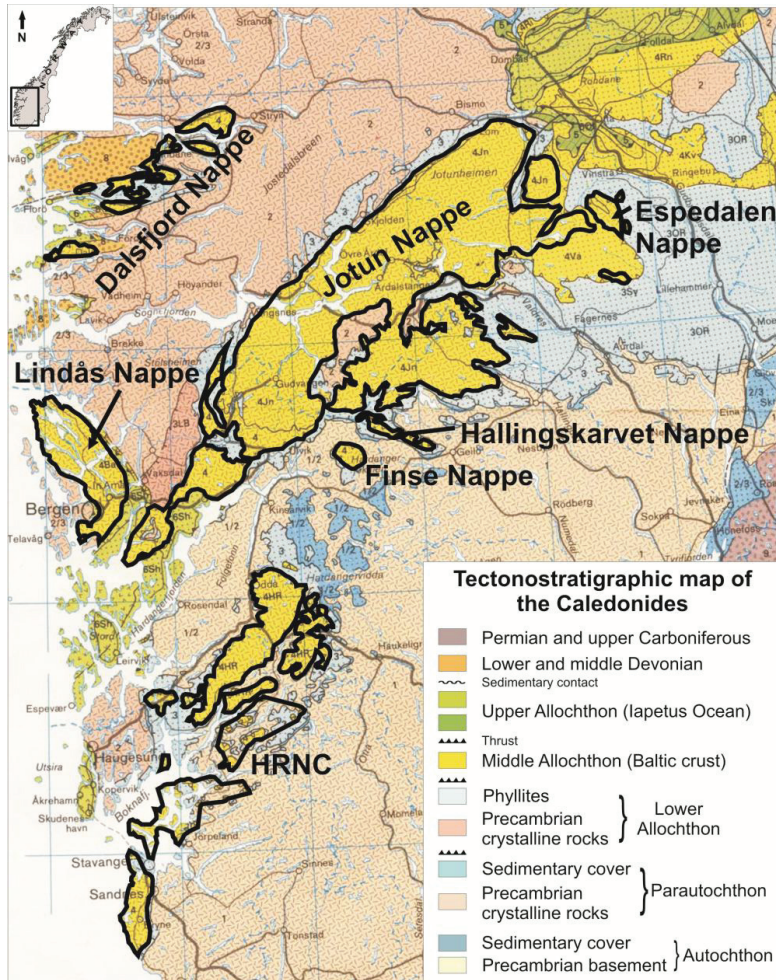


Fig. 4 The SW-Norwegian Caledonides in the tectonostratigraphic map of Norway (after Gee et al. 1985). The main nappes are assigned to the Middle Allochthon (yellow), and are framed and labeled.

3.1. Correlating the nappes

Attempts to correlate the dispersed nappes have a long history. Already Goldschmidt (1916) postulated lithological resemblances between the Jotun-, the Lindås- and the Dalsfjord Nappe.

The crystalline nappes in SW-Norway have indeed many things in common. Consisting mainly of metamorphic intrusives, they generally reveal three main ages reflecting: (1) the protolith age (formation of continental crust), (2) the Sveconorwegian orogenic event (ca 1100-900 Ma) and (3) the Caledonian orogenic event (ca 480-400 Ma). The age of formation of the various units and the extent and timing of metamorphic overprint link nappes to each other and, assuming they derive from the Baltic basement, to a basement terrane. The projection of the present autochthonous basement to the south and west are assumed provenance areas. Provenance studies for the Caledonian event have been done before (e.g. Andresen and Færseth 1982; Bingen et al. 2004; Corfu and Heim 2011; Lundmark et al. 2007; Roberts 2003). The provenance of the Caledonian nappes first and foremost relies on the age of formation of the initial crust. Regarding original age, two major terranes have been identified in the basement in SW-Norway, the Gothian terrane (>1600 Ma, comprising the Sveconorwegian terranes Western Gneiss Region, Idefjorden terrane and Eastern Segment) to the north and east and the Telemarkia terrane (ca 1500 Ma, comprising the Sveconorwegian Telemark-, Rogaland-Agder-, and Bamble-Kongsberg terranes) to the south (Bingen et al. 2005). The response to the Sveconorwegian event in different lithologies further defines and subdivides different locations. The main age distinction during the Caledonian event is between oldest ages (Ordovician, ca 500 to 440 Ma), normally ascribed to nappes with an affinity to the Iapetus Ocean where contraction and HP events occurred before the continent-continent collision, and the Scandian phase (ca 430 to 400 Ma) which are commonly observed in the nappes stemming from the Baltic crust, dating the collision and thrusting of the nappes (Stephens and Gee 1985). However, as mentioned earlier, this general architecture of the nappes is not always coherent with analytical data and observations. The Lindås Nappe, for example, has always been regarded as stemming from the crustal parts of Baltica and has been correlated with the Upper Jotun Nappe due to lithological resemblances, however, it overlies rocks with affinity to the Iapetus Ocean which should be higher up in the tectonostratigraphy (Wennberg et al. 1998). Furthermore, nappes with Gothian terrane affinity and others with

Telemarkian affinity occur in an irregular pattern all over SW-Norway, locally even in the same nappe stack (Corfu and Andersen 2002; Corfu and Heim 2011; paper #2; paper #3), which cannot be explained merely by top to SE thrusting during the Caledonian orogeny. The evident solution for solving these incoherencies is to evaluate in detail the history of all the involved components as a more advanced basis of chronostratigraphic correlation.

This study introduces new U-Pb ID-TIMS age data from smaller nappes in the Finse and Hallingskarvet area, the Lindås Nappe and parts of the HRNC. It also gives a summarized overview and comparison of U-Pb ages from all crystalline nappe sheets in SW-Norway.

4. Introduction to the papers - questions, results and highlights

4.1. Paper #1

Evidence for a Caledonian amphibolite to eclogite facies pressure gradient in the Middle

Allochthon Lindås Nappe, SW-Norway

Published in Contributions to Mineralogy and Petrology, 2012

4.1.1. Facts and open questions:

- The Lindås Nappe has usually been compared to the Upper Jotun Nappe due to lithological similarities. Both largely consist of anorthosite and related intrusives. The stratigraphic position of the Lindås Nappe is, however, obscure since it overlies ophiolitic complexes, assigned to the Upper Allochthon.
- In the central and southern parts of the Lindås Nappe eclogite formed during the Caledonian orogeny along cracks and fluid pathways, whereas eclogites have not been found in the northern part of the Lindås Nappe or in the Jotun Nappe.
- The intrusive age of the anorthosite in the Lindås Nappe is unknown.

4.1.2. Findings and conclusions:

- The northern most part of the Lindås Nappe consists of anorthosite and jotunite, is free of eclogites, and intruded 969 Ma ago.
- Sveconorwegian granulite facies metamorphism dates at 930 Ma, later metasomatic events date at ca 908 Ma.
- Caledonian metamorphism in the north did not exceed amphibolite facies and was contemporaneous with eclogite facies metamorphism further south. The Lindås Nappe is tentatively interpreted to preserve a Caledonian pressure gradient.
- In a shear zone in the anorthosite a case of large (1 mm), low U zircons is recorded, which reacted to deformation with internal deformation and re-crystallization of smaller grains in the pressure shadow, as well as with Pb loss in the old grains.

The U content of the grains is very low, ca 5ppm for the large grains, a bit higher, ca 12 ppm for the small ones in the pressure shadow. Although no metamictisation is seen or expected in such low U zircons, they plot discordantly with an upper intercept of 908 Ma, interpreted as the metasomatic event forming the vein, and a lower, Caledonian intercept (Fig. 5). The Caledonian event is held responsible for the deformation in the vein, causing the growth of the small zircons in the pressure shadow (which date to 426 Ma) of the large ones, and the fracturing and Pb loss in the large grains. Enhanced fluid activity along with the shearing strain during the Caledonian event contributed to the resetting.

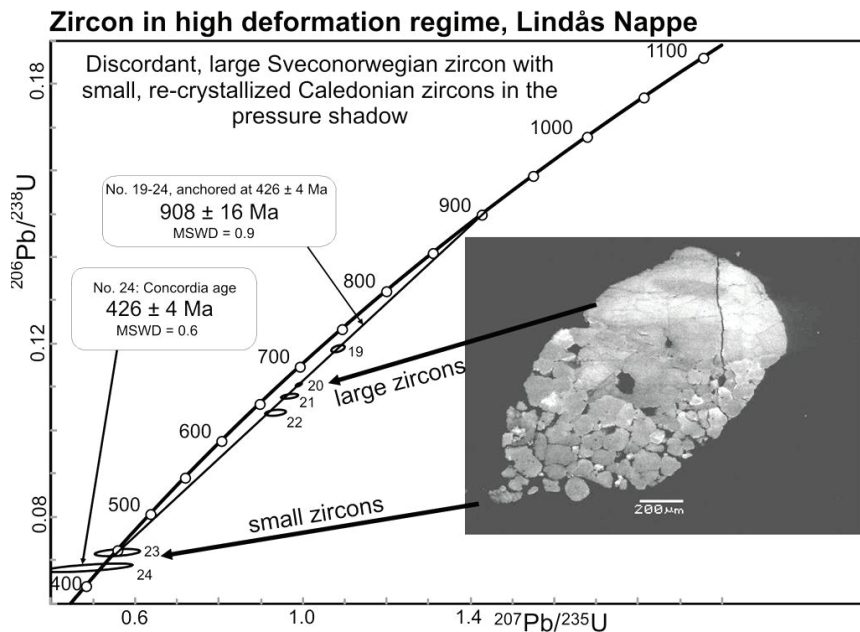


Fig. 5 Large, discordant, low U zircons. The deformation in the large grain is seen on the CL image, the small grains formed in the pressure shadow during deformation.

4.2. Paper #2

A Sveconorwegian terrane boundary in the Caledonian Hardanger-Ryfylke Nappe

Complex: the lost link between Telemarkia and the Western Gneiss Region?

Accepted in Precambrian Research pending major revisions

Currently in the process of being revised

4.2.1. Facts and open questions:

- The HRNC consists of laterally disconnected nappe systems where the largest in the north of the complex consists itself of different nappes.
- Two of these nappes, the Dyrskard and the overlying Kvitenut Nappe, are separated by a shear zone, which was presumed pre-Caledonian in early literature, but analytical proof was missing.
- The different lithologies in the two nappes suggested a different provenance, but no accurate age data was available.

4.2.2. Findings and conclusions:

- The shear zone is Sveconorwegian, giving an age of 999 Ma. A later movement was dated at 926 Ma.
- Dyrskard and Kvitenut have different protolith ages: The Kvitenut Nappe can be assigned to the Gothian terrane with continental growth of > 1600 Ma, the Dyrskard Nappe shows resemblance with Telemarkia and crustal growth at 1500 Ma.
- The boundary between the two basement terranes, the Gothian terrane and Telemarkia, has not been found yet in the west of the Faltungsgaben, but the pre-Caledonian shear zone between Dyrskard and Kvitenut might represent this boundary, hence the nappes might well derive from the western continuation of the boundary of these terranes.

4.3. Paper #3

Correlation of Caledonian crystalline nappes in SW-Norway by means of U-Pb geochronology: old problems and new data

*Prepared for Special Publication of the Geological Society, London:
'New perspectives on the Caledonides of Scandinavia and related areas'*

4.3.1. Facts and open questions:

- Correlation of the crystalline nappes in SW-Norway is not straight forward. Local inconsistencies compared to the general tectonostratigraphic subdivision occur, and from some nappes not enough data are available.
- Age and evolution of two small nappe systems south of the Jotun Nappe Complex, the Finse- and the Hallingskarvet nappes, are largely unknown. The affiliation of the Kvalsida Gneiss next to the Lindås Nappe is in question.
- The phyllite nappes underlying the crystalline nappes in Finse and Suldal (southern part of the HRNC) show infolded layers of metasediments with metarhyolites which are not found elsewhere in a comparable stratigraphic position.

4.3.2. Findings and conclusions:

- Although geographically close, the Upper Finse- and the Hallingskarvet nappes show different protolith ages and evolution. The Upper Finse Nappe shows affinity with the Gothian terrane and hence can be correlated with the Upper Jotun and the Kvitenut nappes. The Hallingskarvet Nappe indicates Telemarkian evolution and is correlated with the Espedalen, Eikefjord and Dyrskard nappes.
- The lower nappes in Suldal and Finse both reveal metarhyolites with an early Sveconorwegian age, the infolded phyllite is therefore considered Precambrian.
- A systematic age profile of the crystalline nappes in SW-Norway with age of formation, Sveconorwegian evolution and Caledonian overprint has been established by using new data and literature data on U-Pb ages.
- Similarities and correlations among the nappes and with the Sveconorwegian basement terranes are pointed out.
- Similar zircon behavior has been detected in some nappes: Zircons from the Upper Finse and the Kvitenut nappes have a discordance pattern in common. The oldest

zircon in these nappes are strongly discordant towards the Sveconorwegian event. The fit on the Discordia line is not good, resulting in a rather high MSWD. It appears that the Caledonian event – although not showing a strong imprint – caused some additional Pb-loss and pulls the analyses slightly down from Discordia. CL images on the zircons show magmatic growth zonations, partly overwritten by re-crystallization and partly surrounded by a low U rim (Fig. 6). Removing the rim with air abrasion could not remove the Caledonian effect on the grains, hence the metamorphic rim is a Sveconorwegian effect. Chemical abrasion, on the other hand, was sufficient to remove the Caledonian effect and results in a better fit. However, also chemical abrasion could not diminish the Sveconorwegian discordance which is therefore regarded as complete re-crystallization of zircon parts.

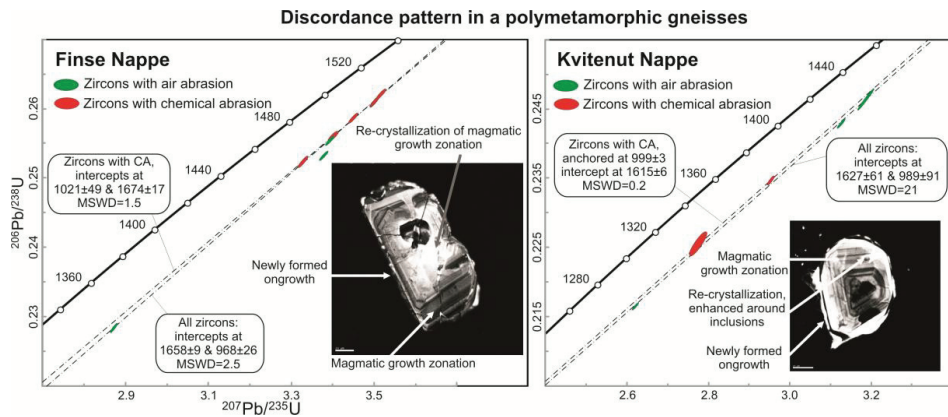


Fig. 6 Same discordance pattern of zircon in two different nappes. Both samples reveal the crystallization age and the Sveconorwegian event. The Caledonian disturbance is only visible in the poor fit along Discordia when using air abrasion (green ellipses) but is diminished when using chemical abrasion (red ellipses).

4.4. Paper #4

Evolution and origin of the Revsegg Nappe in the SW-Norwegian Caledonides: an allochthon with Ordovician elements

*Prepared for Special Publication of the Geological Society, London:
'New perspectives on the Caledonides of Scandinavia and related areas'*

4.4.1. Facts and open questions:

- The Revsegg Nappe, overlying Kvitenut in the HRNC, consists mainly of metapelitic schists with felsic and mafic intrusives, and is strikingly different than the underlying orthogneiss-dominated, crystalline nappes.
- Origin, evolution and the relation to the underlying nappes are largely unclear for the Revsegg Nappe.

4.4.2. Findings and conclusions:

- The contact towards the underlying Kvitenut Nappe is tectonic. Thrusting occurred in the Silurian.
- The intrusives include boudinaged mafic sills, pegmatites and granodiorites. Lenses of metasandstones are found within the metapelites.
- An Ordovician metamorphic imprint is detected in the mafic sills and in the metasandstones. The pegmatites and granodiorites are Silurian but did not intrude contemporaneously, the granodiorites are the latest intrusives.
- The Revsegg Nappe shows affinity with the Iapetus Ocean domain. A tentative correlation with the Upper Allochthonous Jæren Nappe is suggested.

4.5. General conclusions and outlook

The goal of this thesis is to provide new data to fill the holes in the understanding of the structure and correlation of the nappes in SW-Norway. In the process of gathering data, striking cases in terms of geology and/or zircon behavior were found. Some of these cases would provide a good opportunity for follow up research. The most promising one is the complex structure of the lower nappe underneath Finse and Suldal. Little is known about the stratigraphic position of these subunits and their relation to the phyllites in which they are folded in. In general, detailed research on the lower nappes could solve problems like travel path reconstruction of the crystalline nappes during the Caledonian orogeny.

Another interesting question is the distribution and relation of the Ordovician influence in the nappes. The Revsegg Nappe for example shows similarities with the Jæren Nappe, but intrusives in the Jæren Nappe have not yet been dated.

The Caledonides in SW-Norway still provide numerous possibilities for geologists. This thesis hopefully contributes to drawing the interest of many to this manifold area.

References

- Andersen TB, Andresen A (1994) Stratigraphy, tectonostratigraphy and the accretion of outboard terranes in the Caledonides of Sunnhordland, W. Norway. *Tectonophysics* 321:71-84
- Andersen TB, Jamtveit B (1990) Uplift of the deep crust during orogenic extensional collapse – a model based on field studies in the Sogn-Sunnfjord region of Western Norway. *Tectonics* 9:1097-1111
- Andresen A, Færseth R (1982) An evolutionary model for the southwest norwegian Caledonides. *Am J Sci* 282:756-782
- Bingen B, Davis WJ, Hamilton MA, Engvik AK, Stein HJ, Skår O, Nordgulen O (2008a) Geochronology of high-grade metamorphism in the Sveconorwegian belt, S. Norway: U-Pb, Th-Pb and Re-Os data. *Norw J Geol* 88:13-42
- Bingen B, Nordgulen O, Viola G (2008b) A four-phase model for the Sveconorwegian orogeny, SW Scandinavia. *Norw J Geol* 88:43-72
- Bingen B, Skår O, Marker M, Sigmond EMO, Nordgulen O, Ragnhildstveit J, Mansfeld J, Tucker RD, Liegeois JP (2005) Timing of continental building in the Sveconorwegian orogen, SW Scandinavia. *Norw J Geol* 85:87-116
- Bingen B, Austrheim H, Whitehouse MJ, Davis WJ (2004) Trace element signature and U-Pb geochronology of eclogite-facies zircon, Bergen Arcs, Caledonides of W Norway. *Contrib Mineral Petrol* 147:671-683 doi:10.1007/s00410-004-0585-z
- Cherniak DJ, Watson EB, Grove M, Harrison TM (2004) Pb diffusion in monazite: A combined RBS/SIMS study. *Geochim Cosmochim Acta* 68:829-840 doi:10.1016/j.gca.2003.07.012
- Cherniak DJ, Watson EB (2001) Pb diffusion in zircon. *Chem Geol* 172:5-24
- Cherniak DJ (2000) Pb diffusion in rutile. *Contrib Mineral Petrol* 139:198-207 doi:10.1007/pl00007671
- Cherniak DJ, Lanford WA, Ryerson FJ (1991) Lead diffusion in apatite and zircon using ion-implantation and Rutherford backscattering techniques. *Geochim Cosmochim Acta* 55:1663-1673 doi:10.1016/0016-7037(91)90137-t
- Connelly JN (2001) Degree of preservation of igneous zonation in zircon as a signpost for concordancy in U/Pb geochronology. *Chem Geol* 172:25-39
- Corfu F, Andersen TB (2002) U-Pb ages of the Dalsfjord Complex, SW Norway, and their bearing on the correlation of allochthonous crystalline segments of the Scandinavian Caledonides. *Int J Earth Sci* 91:955-963 doi:10.1007/s00531-002-0298-3
- Corfu F, Hanchar JM, Hoskin PWO, Kinny P (2003) Atlas of zircon textures. In: *Zircon* (edited by J.M. Hanchar JM, Hoskin PWO) *Reviews in Mineralogy and Geochemistry*. Mineralogical Society of America 53:468-500
- Corfu F, Heim M (2011) U-Pb geochronology of the Southern Scandinavian Caledonides: The Mesoproterozoic Espedalen anorthosite-gabbro-norite massif and associated rocks. *Mineral Mag* 75:695
- Faure G, Mensing TM (2005) *Isotopes. Principles and Applications*. John Wiley & Sons, Inc., Hoboken, New Jersey
- Fossen H (2000) Extensional tectonics in the Caledonides: Synorogenic or postorogenic? *Tectonics* 19:213-224
- Fossen H (1998) Timing and kinematics of Caledonian thrusting and extensional collapse, southern Norway: Evidence from Ar-40/Ar-39 thermochronology. *Journal of Structural Geology* 20:765-781

- Gee DG, Kumpulainen R, Roberts D, Stephens MB, Thon A, Zachrisson E (1985) Scandinavian Caledonides tectonostratigraphic map. In: Gee DG, Sturt BA (eds) *The Caledonide Orogen-Scandinavia and related areas*, vol. John Wiley & Sons, Chichester, UK, p 1266
- Goldschmidt V (1916) Geologisch-petrographische Studien im Hochgebirge des südlichen Norwegens. In: *Videnskapsselsk Skrift I*, vol Mat-Naturv Kl 2. Uebersicht der Eruptivgesteine im kaledonischen Gebirge zwischen Stavanger und Trondhjem, pp 1–140
- Kylander-Clark ARC, Hacker BR, Johnson CM, Beard BL, Mahlen NJ (2009) Slow subduction of a thick ultrahigh-pressure terrane. *Tectonics* 28 doi:10.1029/2007tc002251
- Lundmark AM, Corfu F, Spurgin S, Selbekk RS (2007) Proterozoic evolution and provenance of the high-grade Jotun Nappe Complex, SW Norway: U-Pb geochronology. *Precambrian Res* 159:133-154 doi:10.1016/j.precamres. 2006.12.015
- Ramberg IB, Bryhni I, Nøttvedt A, Rangnes K (2008) *The Making of a Land*, Geology of Norway. Trondheim
- Reddy SM, Timms NE, Trimby P, Kinny PD, Buchan C, Blake K (2006) Crystal-plastic deformation of zircon: A defect in the assumption of chemical robustness. *Geology* 34:257-260 doi:10.1130/g22110.1
- Roberts D (2003) The Scandinavian Caledonides: event chronology, palaeogeographic settings and likely, modern analogues. *Tectonophysics* 365:283-299 doi:10.1016/s0040-1951(03)00026-x
- Rudnick RL, Gao S (2003) Composition of the Continental Crust. *Treatise on Geochemistry*. 3:1–64
- Scott DJ, Onge MRS (1995) Constraints on Pb closure temperature in titanite based on rocks from the Ungava orogen, Canada - implications for U-Pb geochronology and P-T-t path determinations. *Geology* 23:1123-1126 doi:10.1130/0091-7613(1995)023<1123:copcti>2.3.co;2
- Spear FS, Pyle JM (2002) Apatite, monazite, and xenotime in metamorphic rocks. In: Kohn MJ, Rakovan J, Hughes JM (eds) *Phosphates: Geochemical, Geobiological, and Materials Importance*, vol 48. Mineralogical Soc America, Washington, pp 293-335
- Stacey JS, Kramers JD (1975) Approximation of terrestrial lead isotope evolution by a 2-stage model. *Earth Planet Sci Lett* 26:207-221
- Stephens MB, Gee DG (1985) A tectonic model for the evolution of the eugeoclinal terranes in the central Scandinavian Caledonides. In: Gee DG, Sturt, B.A. (ed) *The Caledonide Orogen: Scandinavia and related Areas*, vol 2. John Wiley, Hoboken, N.J., pp 953-978
- Torsvik TH, Smethurst MA, Meert JG, Van der Voo R, McKerrow WS, Brasier MD, Sturt BA, Walderhaug HJ (1996) Continental break-up and collision in the Neoproterozoic and Palaeozoic -- A tale of Baltica and Laurentia. *Earth-Science Reviews* 40:229-258 doi:10.1016/0012-8252(96)00008-6
- Tucker RD, Robinson P, Solli A, Gee DG, Thorsnes T, Krogh TE, Nordgulen O, Bickford ME (2004) Thrusting and extension in the scandian hinterland, Norway: New U-Pb ages and tectonostratigraphic evidence. *Am J Sci* 304:477-532 doi:10.2475/ajs.304.6.477
- Wennberg OP, Milnes AG, Winsvold I (1998) The northern Bergen Arc Shear Zone - an oblique-lateral ramp in the Devonian extensional detachment system of western Norway. *Norsk Geol Tidsskr* 78:169-184
- White WM (2013) *Geochemistry*. Wiley-Blackwell, in print
- Winter JD (2001) *An Introduction to Igneous and Metamorphic Petrology*. Prentice Hall Inc.

Paper #1

Published in Contributions to Mineralogy and Petrology
164:81-99 doi:10.1007/s00410-012-0727-7

Paper #2

*Accepted in Precambrian Research pending major revisions
Currently in the process of being revised*

A Sveconorwegian terrane boundary in the Caledonian Hardanger-Ryfylke Nappe Complex: the lost link between Telemarkia and the Western Gneiss Region?

C. Roffeis^{a,b}, F. Corfu^a, R.H. Gabrielsen^a

^aDepartment of Geosciences, University of Oslo, Postbox 1047 Blindern, N-0316 Oslo, Norway

^bCorresponding author: cornelia.roffeis@geo.uio.no, tel.: +47 40310430

Abstract

Magmatic and metamorphic events in two of the nappes of the Hardanger-Ryfylke Nappe Complex in the Caledonides in SW-Norway, and in the intervening thrust zone, have been investigated by means of ID-TIMS U-Pb zircon and titanite data. Orthogneiss protoliths in the upper Kvitenut Nappe are dated at 1615 ± 6 Ma, showing analogies to the Gothian terrane, including the Western Gneiss Region. By contrast, the Dyrskard Nappe is composed of metasedimentary rocks and metarhyolites with a 1508 ± 4 Ma extrusion age and shows an affinity to rocks of the Telemarkia terranes. We argue that the time of thrusting and juxtaposition of the two nappes along the shear zone is constrained by the age of 999 ± 5 Ma of a syndeformational granite body and co-genetic pegmatitic leucosomes, with late Sveconorwegian movements and fluid activity being recorded by titanite at 924 ± 6 Ma. Both nappes behaved as one block during the Silurian emplacement in the Caledonian nappe stack, sharing a 434 ± 1 Ma metamorphic peak and later overprints, as young as 414 ± 2 Ma, related to retrogression. The distinct origin and Sveconorwegian age of coupling of the Dyrskard and the Kvitenut nappes suggest that, in their pre-Caledonian location to the west-northwest, they represent the now hidden boundary zone between the Western Gneiss Region and Telemarkia.

Keywords: Caledonides, Sveconorwegian orogeny, U-Pb ID-TIMS geochronology, thrust zone, terrane provenance, zircon

1. Introduction

The geology of southwest Norway was shaped primarily by two main orogenies, namely the Sveconorwegian (ca 1140-900 Ma) and the Caledonian (ca 480-400 Ma), which reworked crust of Mesoproterozoic age. The expressions of the Sveconorwegian event are preserved in the basement of southern Norway, which can be subdivided into several terranes, mainly based on ages of crustal formation and tectonic evolution (Andersen, 2005; Bingen et al., 2005, 2008a, 2008b). Based on protolith ages a division into terranes with an age of ca 1500 Ma (i.e. Telemarkia) and such with ages > 1600 Ma (e.g. Western Gneiss Region, Idefjorden terrane) can be drawn. During the Caledonian orogeny the basement was partially subducted and deformed, and nappes were thrust onto Baltic basement, forming the Caledonian mountain belt. The majority of the Caledonian allochthons in SW-Norway stems from the Baltic crystalline basement, implying a shared evolution with the autochthonous terranes (Gee et al., 1985). However, some Sveconorwegian boundaries, such as the one between the Western Gneiss Region and Telemarkia, are now hidden beneath Caledonian nappes. Therefore, the study of allochthons derived from the outer domains of the original Baltic basement can provide important information for the reconstruction of the Sveconorwegian provinces and their evolution. Following this basic idea we focused on a nappe stack in the area north of Haukelisæter – Røldal, the Hardanger-Ryfylke Nappe Complex (HRNC), which comprises nappes with distinctively different lithologies and evolutions (Fig. 1). The upper part of the succession comprises three nappes, from bottom to top these are the Dyrskard, Kvitenut and Revsegg nappes (Naterstad et al., 1973; Andresen, 1974; Gabrielsen et al., 1979). The region was mapped extensively in the 1970s and early 1980s (Andresen, 1974; Andresen and Færseth, 1982; Gabrielsen, 1976; Gabrielsen, 1980; Naterstad et al., 1973) and Rb-Sr whole rock dating provided evidence of a complex Mesoproterozoic evolution, suggesting, in particular, that a major thrust zone between the Dyrskard and Kvitenut nappes may record Precambrian rather than Caledonian deformation (Gabrielsen et al., 1979). We now have the analytical means to follow up on these early discoveries and establish a time frame for the evolution of the nappe stack as well as investigate the provenance of the nappes. Our results and comparison with the evolution of other allochthonous nappes and autochthonous terranes contribute to a better understanding of the evolution of the Sveconorwegian and the Caledonian orogen.

Throughout this paper we use the term nappe for each Caledonian translated tectonic element, being conscious that the term may need to be adapted as more formal subdivisions are established. The same is valid for the Sveconorwegian orogeny where we refer to the different elements as terranes, following the distinction and nomenclature used by Bingen et al. (2005, 2008a,b). We furthermore use the comprehensive terms “Telemarkia” and “Gothian terrane” for Sveconorwegian terranes with different protolith ages.

2. Geological background

The Caledonian tectonostratigraphy of Norway consists of an autochthonous basement with its Early Paleozoic sedimentary cover overlain by a series of Caledonian thrust sheets. The basement comprises a number of distinct Sveconorwegian terranes, based on the age of crust formation and their specific geotectonic position and evolution during the Sveconorwegian orogeny. A main distinction can be drawn between the Gothian terrane, containing rocks with crustal formation ages of > 1600 Ma, and Telemarkia, comprising terranes with rocks with protolith age of ca 1500 Ma. The Gothian terrane includes the Idefjorden terrane, the Eastern Segment, and the Western Gneiss Region, the latter was highly tectonized by Caledonian events (Fig. 1). Telemarkia comprises the Bamble-Kongsberg, Rogaland-Agder and Telemark sectors (Bingen et al., 2005) (Fig. 7A).

The Caledonian orogeny was caused by the collision of Baltica and Laurentia. The Scandian phase, taking place after closure of the Iapetus Ocean, describes the final collision and the thrusting of nappes onto Baltic basement rocks at ca. 430-420 Ma (Stephens and Gee, 1985; Torsvik et al., 1996). Crustal thickening associated with subduction of the leading edge of Baltica resulted in extensive deformation and metamorphism up to UHP conditions (e.g. Andersen and Andresen, 1994; Cuthbert et al., 2000; Fossen, 2000; Griffin and Brueckner, 1980; Kylander-Clark et al., 2009). The collision was followed by extension and erosion (e.g. Andersen and Jamtveit, 1990; Andersen, 1998; Fossen, 1992; Tucker et al., 2004). Today the Caledonides are represented by a series of allochthons, laterally disconnected by erosion, lying on autochthonous Baltic basement. According to their stratigraphic position and origin, the nappes have traditionally been divided into four units (Gee et al., 1985), consisting of the Lower Allochthon, which represents detached slices of Baltic basement and overlying sediments, the Middle Allochthon, considered to be derived from the outer margin of Baltica, the Upper

Allochthon, interpreted as the outermost margin of Baltica and remnants of the Iapetus Ocean, and the Uppermost Allochthon, inferred to be of Laurentian affinity (Roberts, 2003; Ramberg et al., 2008) (Fig. 1). In detail, this subdivision is somewhat oversimplified, and locally it can be difficult to properly place allochthonous units into this scheme; for example the Kalak nappes in northern Norway have been assigned to the Middle Allochthon (Gee et al., 1985), but based on more recent research they resemble outboard terranes that would normally be assigned to the Uppermost Allochthon (e.g. Corfu et al., 2007; Kirkland et al., 2007; Kirkland et al., 2008). Evidently, the concept of the Caledonides as a sequence of allochthons that can be correlated laterally over vast distances does not always apply.

The problem of correlation is quite evident in the nappes of southern Norway. One classical example is the Lindås Nappe, which based on lithological features has been correlated with the Jotun Nappe, a classical element of the 'Middle Allochthon', yet it apparently overlies Paleozoic arc and ophiolitic elements normally assigned to the 'Upper Allochthon' (Wennberg et al., 1998). The evident approach is to evaluate in detail the history of all the involved components as a more advanced basis of chronostratigraphic correlation.

In southern Norway, the dominant nappes consist of sheets of transposed Proterozoic continental crust overlying allochthonous and parautochthonous metasedimentary successions, in part Paleozoic, but also including Proterozoic elements. The largest crystalline allochthon is the Jotun Nappe Complex, which has similarities with the smaller Lindås and Dalsfjord nappes and the upper part of the Hardanger-Ryfylke Nappe Complex. Most of these nappes are dominated by metaplutonic complexes of various compositions, commonly yielding ages of 1700-1600 Ma, but also including rocks yielding U-Pb zircon ages between 1500 to 950 Ma. In addition to the similarities in age and lithology, the degree of metamorphic resetting during the Sveconorwegian event (ca 1140 - 900 Ma) and the Caledonian event (ca 480 - 400 Ma) also supports a common evolution of different units within the nappes (Bingen et al., 2008b; Lundmark et al., 2007).

2.1. The Hardanger-Ryfylke Nappe Complex (HRNC)

The Hardanger-Ryfylke Nappe Complex overlies Proterozoic autochthonous basement and its autochthonous to parautochthonous sedimentary cover, the Vidda Group (Andresen and Færseth, 1982). The Vidda Group is a shallow marine deposit with fossils indicating Lower

Cambrian to Middle Ordovician deposition. The overlying different nappes in the HRNC are separated by thrust zones, commonly marked by extensive zones of mylonites and blastomylonites. The basal sedimentary unit, named Holmasjø Allochthon, consists mainly of non-fossiliferous gray phyllites and schists. In the eastern domains, the Holmasjø Allochthon is overlain by the Nupsfonn Nappe, a tectonic wedge composed of granitic gneisses and intrusives with local migmatites and an inverted unconformity (Andresen, 1972; Andresen and Færseth, 1982). The lower units are overlain in turn by the Dyrskard, Kvitenut and Revsegg nappes. The Dyrskard and Kvitenut nappes are the subject of this study and are described in more detail below. The uppermost Revsegg Nappe consists dominantly of pelitic metasediments with boudins of quartz, pegmatite and mafic and felsic intrusives. The contact to the underlying Kvitenut Nappe was interpreted as a disturbed sedimentary contact (Jorde, 1973; Naterstad et al., 1973), but is regarded as a tectonized contact by the authors of this study (Roffeis and Corfu, in prep).

2.1.1. The Dyrskard Nappe

The Dyrskard Nappe crops out in western Hardangervidda mainly in the valleys and builds the footwalls of the surrounding mountains (Fig. 2). It can generally be divided into four different units, from bottom to top: (1) banded gneisses and blastomylonites of supracrustal origin, (2) quartzites, feldspathic sandstones and mica schists with minor basic and intermediate metavolcanics, (3) amphibolites with some quartzites and impure marbles and (4) acid metavolcanics, mainly metarhyolite. The basic metavolcanic rocks are restricted to few areas whereas the metarhyolites appear to have been covering the whole nappe and now occur at most of the Dyrskard outcrop locations. Sedimentation and the stratigraphic succession indicate volcanic extrusion and deposition in a calm, continental marginal environment, probably near-shore, and further indicate that the sequence is not inverted (Andresen and Gabrielsen, 1979; Gabrielsen, 1980).

According to Gabrielsen (1980) and Andresen and Færseth (1982), the Dyrskard Nappe rocks were subjected to two metamorphic events. The first one, reaching upper greenschist to lower amphibolite facies conditions, is assigned to the Sveconorwegian event. The second event has been considered to be of lower grade, not exceeding greenschist facies, and restricted to the lower part of the succession, where it is indicated by the breakdown of

amphibole and biotite and new growth of muscovite and chlorite. As we will discuss below, we link leucosome formation, which requires higher metamorphic grades, in the upper parts of the nappe, to Sveconorwegian thrusting. Pegmatites have intruded the gneisses, and are folded to various degrees, together with the main foliation of the gneisses (Fig. 4A). The intrusions therefore appear syndeformational. Two phases of thrusting, with specific deformation features (mainly folds with different orientations), are associated with the metamorphic events throughout the Dyrskard Nappe. The probably most interesting set of folds, with regard to the age of the shear zone towards the Kvitenut Nappe, are open to tight folds with E-W to ENE-WSW trending fold axes with a wavelength of 20-50 cm, concentrated in the mylonitic upper domain of the Dyrskard Nappe. This mylonitic to blastomylonitic part comprises the upper ca 50 m of the Dyrskard Nappe with an upwards increase in strain intensity (Gabrielsen et al., 1979; Gabrielsen, 1980). The folds in this zone may be correlated to the thrusting of the Kvitenut Nappe onto the Dyrskard Nappe. Since superimposed sets of folds occurring throughout the Dyrskard Nappe are considered to be associated with the Caledonian deformation, it was tentatively concluded that the folds in the mylonite zone are older and that the two nappes had already been conjoined prior to the Caledonian event (Gabrielsen, 1980).

The Dyrskard Nappe was first dated by Andresen et al. (1974) who obtained a Rb-Sr whole rock age of 1289 ± 80 Ma. Gabrielsen et al. (1979) analyzed rocks of the thrust zone between the Dyrskard and Kvitenut Nappes by the same method. Samples from the thrust zone, identified as being sheared Dyrskard, gave an array with an apparent age of 1627 ± 114 Ma.

2.1.2. The Kvitenut Nappe

The Kvitenut Nappe lies between the overlying Revsegg and the underlying Dyrskard nappes. The contact to the Dyrskard Nappe is strongly tectonized. The Kvitenut unit is about 100 to 150 m thick but reaches up to 300 m further north. The main rock types are gneisses of dominantly magmatic, but also sedimentary, origin, ranging from quartz-dioritic to granodioritic in composition, which were subjected to and affected by amphibolite facies metamorphism. Locally preserved relics of a mineral assemblage with orthoclase, garnet and pyroxene indicate an earlier, granulite facies metamorphic event. Small granitic intrusions, veins, pegmatites and leucosomes are common in the Kvitenut gneisses, and define an irregular

pattern of intersections. A large granitic intrusive body without apparent deformation fabric, the Stavsnuten granite, occurs in the eastern part of the complex. The border of the granite towards the Dyrskard rocks is also tectonized, containing a sequence of mylonite and blastomylonite. Smaller intrusions of granitic composition mainly occur in the area around the peak of Stavsnuten. A root for the larger intrusive body is not observed despite excellent exposure (Naterstad et al., 1973). Also, no intrusives that can be affiliated with the Stavsnuten granite have been observed to cut the contact to the Dyrskard Nappe (Andresen and Færseth, 1982). All samples from the Kvitenut Nappe used in this study are taken from the area around Stavsnuten (Fig. 3), where most of the Kvitenut succession is accessible and also where the few meters-thick tectonized boundary against the Dyrskard Nappe is best exposed (Gabrielsen, 1976). Blastomylonites and mylonite gneisses are the characteristic thrust zone rocks in the Kvitenut Nappe. They appear to be the more highly deformed equivalents of augen gneisses and granodioritic gneisses at higher levels in the nappe. However, it is important to note that the upper part of the Dyrskard Nappe comprises mylonitic rocks that strongly resemble the Kvitenut thrust rocks (Gabrielsen et al., 1979). Folds with ENE-striking fold axes are common in the thrust zone rocks, and have the same orientation as folds of the upper part of the Dyrskard Nappe mentioned before (Gabrielsen et al., 1979). The thrust zone was regarded to be pre-Caledonian, mainly because of its amphibolites facies metamorphic grade and distinct folds, that are older than Caledonian folds, although the chronological evidence was lacking (Naterstad et al., 1973). The only geochronology carried out on sheared Kvitenut rocks in the thrust zone rocks gave a Rb/Sr whole rock age of 1537 ± 41 Ma (Gabrielsen et al., 1979). Previous dating of gneisses within the Kvitenut Nappe produced a Rb/Sr whole rock age of 1643 ± 88 Ma (Andresen et al., 1974).

3. Analytical Methods

Zircon and titanite were separated using standard crushing, pulverizing, Wilfley table gravity separation, Frantz magnetic separation and heavy liquid. The minerals were hand-picked under a binocular microscope and grouped into fractions or selected as single grains, based on general appearance. For isotope dilution thermal ionisation mass spectrometry (ID-TIMS) U-Pb analysis, zircons were air abraded (Krogh, 1982) or chemically abraded (Mattinson, 2005) and dissolved after addition of $^{202}\text{Pb}/^{205}\text{Pb}/^{235}\text{U}$ spike. Chemical separation of Pb and U

was performed on all fractions except those smaller than 0.004 mg. U and Pb were loaded together with Si-gel and phosphoric acid on Re filaments and measured with a MAT262 mass spectrometer in static mode or, for low signals and all $^{207}\text{Pb}/^{204}\text{Pb}$ ratios, in peak jumping mode using an ion counting secondary electron multiplier. The data were corrected with fractionation factors of 0.1%/amu for Pb and 0.12%/amu for U. Blank correction was 0.1 pg U and 2 pg Pb, or less when the total common Pb was below that level. The initial lead was corrected with the model of Stacey and Kramers (1975). For some titanite fractions with a high amount of common Pb the composition of the initial common Pb was determined using low-U cogenetic titanites. The measured composition of the low-U titanites was corrected for the small amount of accumulated radiogenic Pb and then used as input for the U-bearing titanites. Results from all measurements were plotted and regressed using Isoplot 4.1 by Ludwig (2009). The decay constants are taken from Jaffey et al. (1971). Uncertainties in the isotope ratios and the ages are given and plotted at 2σ .

4. Evaluation of ID-TIMS data

4.1. The Dyrskard Nappe

Due to the general supracrustal character of the rocks of the Dyrskard Nappe, we restricted the geochronological work to a metarhyolite unit (D1), which occupies the top part of the succession, and to pegmatitic intrusions in it (D2, D3). Attempts to find zircon in a gabbroic intrusion in the metasedimentary rocks were not successful.

D1; metarhyolite: The sample was taken from an outcrop close to Valldalsvatnet, where fine-grained gneisses belonging to the metarhyolite sequence are intercalated with pure quartzite on a cm- to dm-scale. Macro- and microscopically clearly visible feldspar phenocrysts reveal the volcanic origin of the gneisses (Fig. 4B). The metamorphic overprint is expressed as a narrow foliation, defined by recrystallized feldspar and quartz alternating with biotite-rich folia. A few idiomorphic garnet crystals, interpreted as metamorphic, are visible in thin section. The major element composition of the volcanic rocks plots in the rhyolitic/rhyodacitic field (Andresen and Gabrielsen, 1979). The sample yielded a large number of zircons, in general showing euhedral, short-prismatic shapes, but commonly broken and metamict. Only grains

and grain pieces with idiomorphic shapes were picked and analyzed after applying air or chemical abrasion.

Single grains or fractions of two grains have been analyzed (Table 1, 1-8). The data points are all somewhat discordant and scatter within a wedge shaped area (Fig. 5) between regression lines trending towards either a Sveconorwegian or a Caledonian age. It is therefore likely that the zircons have been affected by both orogenies. Various combinations of data points, anchored at either a Caledonian or a Sveconorwegian event, converge towards similar upper intercept ages of ca 1493-1508 Ma. Analyses (1) and (2) have the highest $^{207}\text{Pb}/^{206}\text{Pb}$ ages and fit on a discordia line, anchored at 430 ± 3 Ma, providing an upper intercept age of 1508 ± 4 Ma (MSWD=0.27) which is interpreted to date the volcanic event. From a technical point of view it is interesting to note that with this sample chemical abrasion yielded more discordant analyses than air abrasion, although the difference does not affect the general data pattern. It may suggest that the zircon grains have been affected by the younger events mainly in the outside domains, which were then removed by air abrasion.

D2; pegmatite in metarhyolite: The pegmatite is folded and part of a suite of dikes cutting metarhyolites. The variable deformation of the pegmatite and the surrounding suggests syntectonic emplacement (Fig. 4A). The sample contains just few zircon grains, but titanite occurs in significant amounts (Table 1, 9-15). Many titanite grains show well developed crystal shapes and are colorless. The zircon population comprises idiomorphic, largely metamict grains or tips of grains with [101] pyramidal faces, and a second population of clear, anhedral grains. A single grain analysis from a metamict zircon (9) gives a discordant age which, when anchored at the Caledonian event at 430 ± 3 Ma, has an upper intercept at 1456 ± 5 Ma. The second analysis of a clear zircon grain (10) plots concordantly at 1225 Ma. Both grains are regarded to be xenocrystic. Four titanite analyses (11, 12, 13, 14) plot concordantly indicating Caledonian ages. Three of the data points overlap within error (12, 13, 14) and give a Concordia age of 414 ± 2 Ma. One titanite fraction (11), however, plots higher on Concordia, at ca 450 Ma, suggesting the presence of a relict earlier titanite generation. This may imply that the pegmatite is pre-Caledonian, perhaps the same age as the pegmatitic vein discussed below, in which case the titanite would reflect Caledonian metamorphism. Nevertheless, a Caledonian age of emplacement cannot be totally excluded.

D3; pegmatite in gneiss: The pegmatite occurs as dm-sized dikes, subconcordant to the main fabric and gently folded. The host rock is a fine-grained pink gneiss with local schistose

intercalations, which has developed thin, highly folded neosome veins. Although a volcanic origin is not as obvious as in the metarhyolite outcrops, Gabrielsen (1976) favored the possibility that also these fine grained gneisses are metavolcanic derivatives. Only a few zircon grains were found in the sample. Small, clear grains show mainly a short prismatic shape, but are subrounded and some cores are visible. Larger grains and tips of grains have a better developed euhedral shape, are dominated by [101] pyramidal faces and are metamict. These are presumably the zircons that crystallized in the pegmatite whereas the clearer, subrounded grains are most likely xenocrystic. Four analyses of grains representing the clearer varieties plot in the same wedge-shaped area, between ca 1000 and 1500 Ma, as defined by the zircons from the metarhyolite, consistent with a xenocrystic origin from the surrounding host rocks (Table 1, 16-19). Two of these analyses (16, 19) fit on a line between 1508 and 985 Ma. Two other grains (20, 21) representing the brown, metamict, euhedral zircons are also discordant, but plot on a very different line with Sveconorwegian and Caledonian intercept ages, defining an upper intercept at 985 ± 4 Ma and a lower intercept age of 412 ± 8 Ma. Because of the magmatic characteristics of the metamict, euhedral zircons, the age of 985 Ma is interpreted to represent the age of formation of the pegmatites. The lower intercept at 412 ± 8 Ma is in accordance with the age of titanite in pegmatite D2. Titanite in D3 (22) is colorless with a relatively low amount of U (26 ppm U) but with relatively high common Pb (for titanite; 16 ppm). The corrected analysis, using the initial Pb isotopic composition of a second low-U titanite fraction (23), is concordant at 403 ± 5 Ma, younger than the zircon intercept and titanite in pegmatite D2. These characteristics suggest that the titanite might be a late metamorphic product of retrogression.

4.2. The Kvitenut Nappe

All samples from the Kvitenut Nappe are taken from the area around Stavsnuten (Fig. 2, 3). On this mountain, the Kvitenut Nappe provides continuous outcrops from the basal thrust above the Dyrskard Nappe upwards, but it does not reach the contact to the Revsegg Nappe. The samples derive from different lithologies at different tectonostratigraphic levels. Sample K1 represents one of the coarse granodioritic augen gneisses, typical for large parts of the complex, although in detail most outcrops show considerable complexity with deformation and cross-cutting dikes. Sample K2 is an amphibolite gneiss interlayered with, and perhaps cut by

the granodioritic rocks. The thrust zone at the base of the Kvitenut Nappe consists of 5-10 m thick blastomylonitic gneisses with distinct feldspar augen referred to as mylonitic augen gneisses (cf. Fig. 4 in Gabrielsen et al., 1979; Fig. 4C). The strongly deformed rocks are lithologically similar to rocks at a higher level within the complex, one of which is represented by sample K1. The mylonitic augen gneisses were sampled in two areas, marked as K3 and K4 in Figs. 2 and 3. Sample K5 stems from the Stavnuten granite at the eastern border of Kvitenut and K6 is a pegmatitic leucosome.

K1; augen gneiss within the Kvitenut Nappe: The augen structure of this rock is defined by folia of biotite wrapping around large feldspar grains, and alternating with bands of fine-grained feldspar and quartz neoblasts. Also co-genetic with biotite are epidote, muscovite and large, up to 1 mm, titanites. Zircons in this sample are mainly prismatic, but most of them exhibit some degree of subrounding. Five analyses (Table 1, 1-5; Fig. 6) are all highly discordant and aligned along a discordia line with an upper intercept at 1627 ± 61 Ma and a lower intercept at 989 ± 91 Ma, but with poor fit (MSWD=21), indicating primary crystallization at about 1630 Ma, and a severe resetting during the Sveconorwegian event. The zircons have evidently not been affected very strongly by the Caledonian events, but the poor fit probably reflects a weak disturbance at that time. Two of the analyses were obtained with chemical abrasion and they fit on a line passing through 999 ± 5 Ma (Sveconorwegian age, see below) yielding an upper intercept of 1615 ± 6 Ma, whereas those treated only with air abrasion fall slightly below this line, possibly reflecting incomplete removal of material affected by Caledonian Pb loss. Interestingly, chemical abrasion in this case did not manage to reduce the Sveconorwegian discordance, suggesting that it was caused by extensive recrystallization of the zircons, compatible with the assumed high-grade (granulite-facies) metamorphism.

K2; amphibolite gneiss: The main minerals are feldspar, biotite and amphibole and sporadic epidote-zoisite. Titanite is abundant and in equilibrium with biotite, forming the foliation. Zircon analyses in this sample scatter due to superimposed Sveconorwegian and Caledonian events (Fig. 6). Therefore, a meaningful regression line cannot be determined. The oldest analysis (6) fits on the line defined for sample K1, suggesting a comparable origin. Three other grains (7-9) yield approximately Sveconorwegian positions in the Concordia plot. Two are discordant (8-9) and have older $^{207}\text{Pb}/^{206}\text{Pb}$ ages than analysis 7, which is slightly reversely discordant with a $^{206}\text{Pb}/^{238}\text{U}$ age of 961 ± 10 Ma suggesting growth of zircon at this time. Titanite comprises two types, distinguishable in color. A brown, high-U grain (10) plots

discordantly with a $^{206}\text{Pb}/^{238}\text{U}$ age of 858 Ma whereas a fraction of pale and U-poor titanite grains (11) is much more discordant with a $^{206}\text{Pb}/^{238}\text{U}$ age of 568 Ma, implying growth of a new Caledonian titanite generation, but still with an inherited component. Projected from a Caledonian age, the titanite data define an upper intercept age of 921 ± 15 Ma, which dates early titanite growth.

K3; augen gneiss, base of the Kvitenut Nappe: The general mineralogy and texture of the sample strongly resemble those of augen gneiss K1, except that K3 shows an even stronger blastomylonitic texture with large feldspar augen, wrapped around by fine-grained feldspar, quartz and biotite forming the metamorphic banding. This structure demonstrates higher strain at the base than within the nappe. Few garnets and old, larger biotite grains occur. Zircon is abundant and present in all bands, also together with the feldspar clasts, whereas titanite is restricted to biotite rich, recrystallized domains. Most zircon grains are either subrounded or metamict. Three analyses (12-14) plot discordantly, a metamict grain (14) being the most discordant one. The scatter of the data points suggests an influence by both the Sveconorwegian and the Caledonian events. The analysis of the least rounded grain (12) however, when anchored at the established 999 ± 3 Ma age of the granite (K5), gives an upper intercept of 1603 ± 7 Ma. The data point also falls on a regression line with those of the chemically abraded zircons from K1 (3, 4) giving intercepts at 974 ± 19 Ma and 1601 ± 8 Ma (MSWD=0.78).

K4; augen gneiss, base of the Kvitenut Nappe: The main reason for examining this sample was to constrain the age of thrusting. Therefore, we focused on the analysis of titanite, which occurs in great number in this sample and can be divided into small (<200 μm) pale, and larger (>200 μm) orange colored grains. In thin section the large, colored titanites are in equilibrium with biotite and recrystallized quartz and feldspar, which now form the augen-structure (Fig. 4D). A CL image of one of these titanites shows only slight recrystallization at the tips but otherwise a homogeneous grain (Fig. 4E). Therefore, we consider the large titanites to have formed during the blastomylonitic event.

Analyses of both titanite types reveal that they belong to two generations. The pale titanite has only about 1 ppm or less U. A fraction of four clear, prismatic grains (18) contained mostly common Pb, which was used for common Pb correction on a second fraction of pale titanites (17) that had a little more U. After Pb correction, this sample plots concordantly at 421 ± 9 Ma, clearly a Caledonian age. In contrast, the orange grains (15, 16) are U-rich and plot

close to Concordia around the Sveconorwegian event. The best analysis (16), anchored at the Caledonian age given by the pale titanites, gives an upper intercept of 924 ± 6 Ma, the second analysis of an orange grain (15) plots slightly reversely discordant, presumably related to the extremely high U content of 1640 ppm of this grain. In accordance with thin section observations we tie the older titanite to the thrusting, which thus happened during the Sveconorwegian event. The Caledonian overprint, however, also formed new titanite, probably during retrogression. Small, marginal recrystallization on the large titanites is also regarded as a Caledonian effect, in the data visible as slight discordance (16).

K5; Stavsnuten granite: The granite outcrops at the eastern end of the Kvitenut Nappe in the study area. At the border towards the underlying Dyrskard Nappe the granite is deformed by the basal thrust and forms blastomylonites. Away from the thrust zone the granite shows only weak deformation and some variation in grain size, but is in general rather homogeneous. The main components are white feldspar, which appears pink when weathered, and gray quartz, in addition to small amounts of both dark and light mica.

Zircons are abundant and vary in shape and appearance. Mainly tips of grains and entire, prismatic grains were analyzed. The majority of the data points cluster around ca 1000 Ma (Fig. 6), with one long prism (28) being more discordant towards younger ages and two grains (20, 19) plotting discordantly but with older $^{207}\text{Pb}/^{206}\text{Pb}$ ages than the rest. The latter grains did not have the typical euhedral crystal shapes and are most likely xenocrystic. These analyses define a line with an upper intercept age of 1483 ± 14 Ma, which may represent the age of the source of the magma, and a lower intercept age of 995 ± 6 Ma. The discordant younger analysis of a long prismatic, clear grain (28), when anchored at 430 Ma defines a discordia line with an upper intercept of 992 ± 7 Ma. Three fully concordant analyses (21, 23, 25) yield a Concordia age of 999 ± 5 Ma. Four other data points (22, 24, 26, 27) overlap within error with these three analyses but not with the Concordia curve. This moderate heterogeneity in the distribution of the data is likely a result of both some Pb-loss and slight amounts of inheritance. The age of 999 ± 5 Ma is considered the best estimate for the intrusion of the granite.

K6; pegmatitic leucosome: Leucocratic veins are common in gneisses of the Kvitenut Complex. The rims of the veins are blurred, and they build a complex network of intersections. It can, therefore, not always be determined with certainty whether the veins represent in situ leucosomes, pegmatites, or both, intersecting and following each other. The main minerals in

this sample are cm-sized, idiomorphic feldspars and smaller quartz. Epidote-zoisite and chlorite occur along cracks. Zircons in this sample mostly have [101] pyramidal faces, typical for zircons in pegmatites. Whole zircon grains and tips with well developed euhedral shapes were chosen for analysis. Two analyses (29, 30) plot at the Sveconorwegian event, the other two (31, 32) at the Caledonian event. The older grains are higher in U, but otherwise no systematic relationships between age and shape can be observed. A regression line with all four data points reveals intercepts at 423 ± 30 and 993 ± 17 Ma (MSWD=9.3). One clear tip of a grain (29) plots slightly to the left of Concordia but still partly on it and gives a Concordia age of 989 ± 4 Ma. Metamict tips (30) are slightly discordant and, when anchored at 430 Ma, give an upper intercept of 995 ± 3 Ma. That is consistent with the intrusive age of the Stavsnuten granite body. New zircon growth at the Caledonian event is indicated by clear tips (31), plotting concordantly at 434 ± 1 Ma. A prismatic grain (32) is slightly discordant and younger.

5. Discussion

5.1. Protolith ages of the Dyrs kard and Kvitenut nappes

The metarhyolites of the upper part of the Dyrs kard Nappe yield a well defined age of 1508 ± 4 Ma, and so far there is no other zircon evidence pointing to the presence of much older crustal components in this nappe. It thus contrasts greatly with the overlying Kvitenut Nappe where the typical orthogneisses indicate crystallization at least 100 Ma earlier at about 1615 ± 6 Ma. Similar age components are present in the other Kvitenut samples investigated, suggesting a common origin. That implies a different provenance of the Dyrs kard and Kvitenut nappes.

5.2. Correlation of the nappes with other allochthonous and autochthonous elements

The Dyrs kard Nappe with the 1508 ± 4 Ma metarhyolites, in combination with the lithological association to quartzites, local marbles and metabasaltic rocks, and similar major element chemistry of the metarhyolites (Andresen and Gabrielsen, 1979), shows great similarity to the metarhyolites in the Rjukan and overlying Vemork groups, part of the "Telemark supracrustals", which are presently found in the autochthonous basement

underneath and surrounding the Hardanger-Ryfylke Nappe Complex (Fig. 7). These rocks have been dated at ca. 1510-1495 Ma (Dahlgren et al., 1990; Laajoki and Corfu, 2007). However, since the general thrusting direction during the Caledonian orogeny was roughly to the southeast, the nappes must have originated west of their current position. The Rogaland-Agder sector (Fig. 7), part of Telemarkia and covering large parts of southwest Norway, comprises rocks ca 1500 Ma old (Bingen et al., 2005) and a former extension further west may well have been the source for the Dyrskard Nappe. To the west of the study area, autochthonous "Telemarkia" metarhyolites occur (Torske, 1982; Bingen et al., 2005)

Among the other nappes of SW Norway, the only one with an equivalent age as Dyrskard is the Espedalen Complex, a subnappe of the Jotun Nappe Complex. Zircons in a noritic anorthosite in this complex gave an age of 1521 ± 9 Ma, and a lamprophyre dike yielded 1514 ± 7 Ma (Corfu and Heim, 2011). In earlier literature a tentative correlation, based on lithology, between Dyrskard and the Bergsdalen Nappe was also discussed (Gabrielsen, 1980; Naterstad et al., 1973). The sedimentary sequence is comparable, apart from conglomerates, which occur in the Bergsdalen Nappe but are missing in the Dyrskard Nappe. However, it was considered that such lithologies might have been present in the sedimentary succession in Dyrskard as well, but sheared off following one of the thrusting events (Gabrielsen, 1980). Nevertheless, the age of 1508 Ma for the metarhyolites obtained in the present study does not match a 1219 ± 111 Ma Rb/Sr age of metarhyolites in the Bergsdalen Nappe (Gray, 1978). A relation of Dyrskard rocks to similar metarhyolites within the phyllites of the Lower Allochthon in the Suldal area to the southwest of the HRNC, has been considered in the past (Andresen and Gabrielsen, 1979; Kildal, 1973), but can be disregarded, since the Suldal rocks are clearly younger. A U-Pb zircon age of about 1040 Ma (Roffeis and Corfu, in prep) confirms and refines the earlier Rb/Sr whole rock age of 1145 ± 98 Ma (Sigmond and Andresen, 1976).

The Kvitenut rocks, on the other hand, with an assumed primary age of over 1600 Ma, would suggest a provenance more to the northwest of SW-Norway. Baltic basement with 1700-1600 Ma ages is the dominant component of the Sveconorwegian terranes east of Telemarkia and of the Western Gneiss Region (e.g. Gaal and Gorbatshev, 1987; Skar et al., 1994; Tucker et al., 1987). Basement with 1700-1600 Ma ages is also an important constituent of the Jotun Nappe Complex (Schärer, 1980; Lundmark et al., 2007) as well as documented in the Dalsfjord Nappe and the Hardangerjøkulen klippe (Corfu and Andresen, 2002; Roffeis and Corfu, in prep).

5.3. The Sveconorwegian evolution

An important similarity between the Dyrskard and Kvitenut nappes and other crystalline nappes of southwestern Norway is the pronounced Sveconorwegian overprint in terms of magmatic activity, deformation and metamorphism. Typical consequences in rocks of all these nappes are the strong Sveconorwegian isotopic resetting of older zircon, in part with Sveconorwegian new zircon growth, and almost ubiquitous isotopic resetting and new growth of titanite. Thus, these nappes clearly must have been derived from parts of the Sveconorwegian orogen now forming the basement underneath the Caledonian Allochthons. The nappes can thus be assigned to the Sveconorwegian terranes in terms of provenance, a subdivision to which terrane is mainly based on the age of crustal formation, but also on the timing and nature of the Sveconorwegian overprint.

In the Dyrskard Nappe Sveconorwegian metamorphism was described to be of medium grade (Gabrielsen, 1980). Our observations of metamorphic garnet growth in the metarhyolites and partial melting/leucosome formation in metapelitic and metavolcanic gneisses suggest at least amphibolite facies. The event is dated by the concordant pegmatitic veins at 985 ± 4 Ma. These veins occur more frequently in tectonostratigraphically upper parts of the nappe, where the surrounding lithologies also show gradually increasing deformation into mylonitic rocks where the thrust zone is approached (Gabrielsen et al., 1979). The increasing deformation, the leucosome formation and veins are tentatively correlated to the thrusting of the Kvitenut over the Dyrskard Nappe.

In the Kvitenut Nappe the Sveconorwegian events caused: (1) very strong resetting of zircon in the orthogneisses (K1 and K3); (2) intrusion of the Stavsnuten granite (999 ± 5 Ma) (K5); (3) development of leucosomes (993 ± 17 Ma) (K6); (4) development of the distinct 5-10 m blastomylonitic thrust zone separating the Kvitenut from the Dyrskard Nappe (age to be discussed below) (K3 and K4); and (5) new growth of titanite (924 ± 6 Ma) (K2 and K4). The marked discordance of the zircon data was the response to Sveconorwegian high grade metamorphism. Chemical abrasion removed the minor Pb loss effects of the Caledonian metamorphic overprint, but it did not diminish the Sveconorwegian U-Pb resetting. Therefore, we consider that the resetting was caused by extensive recrystallization of the zircons (Cherniak and Watson, 2001; Connelly, 2001), manifested in the slight rounding of originally idiomorphic zircons and seen on CL images, observed in K1 (Fig. 6). That would require high

metamorphic conditions such as granulite facies during the Sveconorwegian event, which is documented by remnants of garnet-pyroxene-orthoclase parageneses in some of the Kvitenut rocks (Gabrielsen, 1976). Growth of titanite is another expression of metamorphism, but based on the age it appears to have been mainly a product of a later Sveconorwegian stage, as will be discussed below. The metamorphism was associated with local partial melting and the development of diffuse leucosomes. The result of 993 ± 17 Ma obtained from the pegmatitic leucosome K6 reflects this melting stage. The leucosomes were contemporaneous with the intrusion of the Stavsnuten granite at 999 ± 5 Ma (K5).

5.3.1. Sveconorwegian thrusting of the Kvitenut onto the Dyrs kard Nappe

The thrust zone at the base of the Kvitenut Nappe is 5-10 m thick, consisting of blastomylonitic gneisses, equivalent, but subjected to a higher deformation intensity than gneisses higher up in the succession. The thrust effect in the Dyrs kard Nappe is seen as a gradual increase of strain in the upper approximately 50 m thick zone of the Dyrs kard rocks (Gabrielsen et al., 1979). The age of the shear zone is constrained by two events: (1) The 999 ± 5 Ma Stavsnuten granite is sheared at the base, implying that the thrust has to be younger, and (2) large titanite, which is in equilibrium with minerals forming the blastomylonitic texture in the shear zone, give an age of 924 ± 6 Ma. Another feature, below the sheared base of Kvitenut but within the broader zone of thrust related highly deformed rocks at the top of the Dyrs kard Nappe, are leucosomes and pegmatites. They are syndeformational and increase gradually in abundance towards the boundary with the Kvitenut Nappe. Similar leucosomes occur in the Kvitenut rocks. Both yield early Sveconorwegian ages, 985 ± 4 Ma (D3) for Dyrs kard rocks and 993 ± 17 Ma (K6) for a pegmatitic leucosome derived from the Kvitenut Nappe. Considering the accumulation of the leucosomes towards the thrust zone in each nappe, those features can be related to the thrusting. The titanite must then have grown during a later movement. Alternatively, the leucosome formation as well as the granulite facies metamorphism were not related to the thrusting but to an earlier event that affected both nappes to the same extent. That would place the nappes in the same area at this time but not yet on top of each other. In that case the age of thrusting and juxtaposition would be given by the titanite and date at 924 ± 6 Ma. We also note, however, that titanite in the amphibolite gneiss well above the main thrust at the base of the Kvitenut Nappe gives a similar age of 921 ± 15 Ma, suggesting that this

event can be detected not just in the shear zone but also elsewhere in the nappe and might e.g. reflect late resetting related to a hydrothermal overprint, or to late Sveconorwegian extension which is seen in the Mylonite Zone between the Idefjorden terrane and the Eastern Segment (e.g. Bingen et al., 2008b and references therein). Titanite formation at that time is also seen in other nappes, like the Finse and Hallingskarvet nappes, to the north of the study area (Roffeis and Corfu, in prep.). Another interesting point is the fact that inherited zircons present in the Stavsnuten granite do not have the 1600+ Ma age of the Kvitenut Nappe, but point instead to an age of 1483 ± 14 Ma, which corresponds rather to the age of the Dyrs kard rocks. This suggests that the granite was generated by melting of Dyrs kard-type rocks, but before final emplacement, since there are no equivalent large granite masses in the presently exposed parts of the Dyrs kard Nappe. This would furthermore imply emplacement of the granite during thrusting over Dyrs kard-type rocks. Putting all these information together we argue that the main thrusting occurred at around 1000 Ma, but it was likely a protracted multistage process, and the more narrow thrust plane was at least reactivated at 924 ± 4 Ma, with formation or final shaping of the presently observed mylonitic gneisses (Fig. 4C and D), including growth of titanite.

5.4. The Caledonian event and emplacement of the nappes

Since the thrusting happened during the Sveconorwegian event, both nappes have been transported together during the Caledonian event. The Caledonian event is not as pronounced as the Sveconorwegian event, the dominant mineral paragenesis are Sveconorwegian. In the zircons Caledonian metamorphism partly led to discordance (seen in all samples) and formation of new zircon in one sample (K6). It also led to the formation of titanite grains and partial recrystallization of older titanite (K2, K4, D2, D3). Caledonian peak metamorphism is revealed by zircon whereas titanite formation is related to later retrograde overprints. Concordant idiomorphic Caledonian zircons with an age of 434 ± 1 Ma are found in the pegmatitic leucosome K6 in the Kvitenut Nappe. The sample also comprises Sveconorwegian idiomorphic zircons, which we have interpreted above as having crystallized during the original synmetamorphic emplacement of the pegmatite. Both zircon populations have the appearance normally associated with primary magmatic crystals and only differ in U-content. Since both zircon populations apparently date an intrusive event, we consider the

possibility that a Sveconorwegian pegmatite became the locus of renewed partial melting which subsequently crystallized forming new zircon during the Caledonian event. The lower U-content in the younger zircons would be consistent with that theory. However, one could argue that such a melting event should affect the partly metamict, old zircons to a higher degree. A second possibility is that the sample was taken at an intersection of two pegmatites or a pegmatite and a leucosome. The gradational rims and unclear intersection patterns of pegmatites and leucosomes throughout the Kvitenut Nappe make this possibility plausible.

Caledonian titanite in two samples reveal younger ages than given by zircon: 421 ± 9 Ma for titanite in the thrust zone and 414 ± 2 Ma for titanite in the two pegmatites of the Dyrs kard Nappe. These titanites are pale and considerably lower in U than the Sveconorwegian titanites, and are, therefore, tentatively interpreted to be related to a late Caledonian retrograde overprint. In the case of titanite from the thrust zone it could be questioned as to whether the Caledonian titanite may be related to reactivation of the thrust. However, the fact that the coexisting large, Sveconorwegian, U-rich titanites are not very strongly reset argues against that.

5.5. Provenance studies

A crude distinction into basement terranes based on the age of crustal formation has been introduced above. In addition there are some very significant distinctions concerning the exact timing of the Sveconorwegian events. As discussed above, the Kvitenut and Dyrs kard nappes were affected by magmatism and metamorphism mainly in the period 1000 to 960 Ma, especially with intrusion of the 999 Ma Stavs nuten granite and coeval or slightly younger leucosomes and pegmatites in the two nappes, likely also reflecting the main period of thrusting, juxtaposition of the two nappes and metamorphism. This period corresponds to the final stages of the main Sveconorwegian Agder phase (1050-980 Ma) in the model of Bingen et al. (2008b), a period related to tectonic imbrication and crustal thickening recorded especially in the core of the orogen, and possibly linked to continental collision. The closest analogue found so far in the basement in the southern part of the Western Gneiss Region is granulite facies rocks metamorphosed at 987 ± 10 Ma (Røhr et al., 2004). Further north in the Western Gneiss Region, high-grade metamorphism and granitic magmatism occurred at a later stage (around 960-950 Ma; Skår and Pedersen, 2003; Glodny et al., 2007). However, the record of a

similar age in the basement terranes is given by two samples from the Åmot-Vardefjell shear zone, a border between Telemarkia and the Idefjorden terrane (Gothian terrane) (Bingen et al., 2001; Bingen et al., 2008b), where zircon in amphibolites facies banded gneisses reveal metamorphism, probably related to thrusting, in the Agder phase (1008 ± 14 and 1012 ± 7 Ma).

In other allochthons of southern Norway a corresponding ca. 1000 Ma metamorphic overprint has only been recorded in the Espedalen Complex, which, as mentioned above, is also the only known allochthon generated at about 1500 Ma and equivalent to the Dyrskard Nappe.

The other main nappes of southern Norway, the Jotun, Dalsfjord and Lindås nappes, are distinctly different with respect to the Sveconorwegian evolution. As far as we presently know, the bulk of the Lindås Nappe was generated by magmatic events mainly between 980 and 950 Ma and was affected by multiple stages of high-grade metamorphism between 950 and 910 Ma (Roffeis et al., 2012, and references therein). Hence, large parts of the Lindås rocks did not yet exist at the time of the main transformations and thrusting of the Dyrskard and the Kvitenut nappes. Similarly, the Jotun and Dalsfjord nappes underwent their major magmatic, deformational and metamorphic phases only after 970 Ma and as late as 900 Ma (Schärer, 1980; Corfu and Andersen, 2002; Lundmark et al., 2007; Lundmark and Corfu, 2008). Also large anorthosite intrusions, which are the main components of the Lindås and the Jotun Nappe Complex, are missing in the Kvitenut and Dyrskard nappes. This final stage of the Sveconorwegian orogeny is named the Dalane phase in Bingen et al. (2008b), who interpret it as reflecting extension and gravitational collapse of the orogen. In the autochthon, the event is recorded mainly in two terranes, the Eastern Segment, which underwent exhumation following high pressure metamorphism (Bingen et al., 2008a, 2008b), and in Rogaland-Agder with emplacement of the Rogaland Anorthosite Complex and associated metamorphism at 930 Ma (Bingen and van Breemen, 1998; Schärer et al., 1996). In addition, at about that time the orogen was intruded by suites of late granitic plutons (e.g. Andersen et al., 2002; Bingen et al., 2008b). The only evidence of a late Sveconorwegian overprint in the Dyrskard and Kvitenut nappes is the formation of titanites in the sheared boundary and in the amphibolite in the Kvitenut rocks at 924 ± 6 Ma and 921 ± 15 Ma, respectively. They probably reflect reactivation of the shear zone and fluid activity in the upper crust during the Dalane phase.

5.5.1. Reconstruction of the pre-Caledonian arrangements

The emerging specific temporal relationships between different allochthons and between these and the subdivisions of the autochthonous basement can be used to reconstruct the pre-Caledonian architecture and structures in the western domains of the Sveconorwegian orogen. An illustration of the main autochthonous terranes is shown in Fig. 7. The inferred, pre-Caledonian and pre-Sveconorwegian thrusting location of the Kvitenut and Dyrs kard nappes is based upon age correlation. Our data would place Kvitenut rocks to the west of the Western Gneiss Region and the Dyrs kard Nappe further south at the western continuation of Telemarkia (Fig. 7B). The thrusting occurred at 999 ± 5 Ma, with the thrust zone between the Kvitenut and Dyrs kard nappes representing the boundary between the Gothian terrane and Telemarkia (Fig. 7B). The 999 Ma Stavs nuten granite in the Kvitenut Nappe contains 1500 Ma inherited zircons. That could indicate that the granitic melt was generated in, or traveled through, a 1500 Ma terrane. Taking into consideration the previously mentioned discrepancies between the Kvitenut rocks and other 1600 Ma terranes, one could speculate that the Kvitenut Nappe was no longer part of the Gothian terrane at 999 Ma, but already in transit over 1500 Ma Telemarkian rocks. During the subsequent Caledonian orogeny both nappes were transported as one block. The main direction of thrusting for Caledonian nappes on Baltica is from NW to SE (Fig. 7B).

Other terrane boundaries, like the above mentioned Åmot- Vardefjell shear zone, or the Mylonite zone between the Eastern Segment and the Idefjorden terrane are usually wide shear zones with thicknesses in a km range, and also usually not subhorizontal but steeply dipping (Bingen and Solli, 2009; Bingen et al., 2001; Stephens et al., 1996). The narrow and subhorizontal shear zone between the Kvitenut and the Dyrs kard nappes does not resemble those, perhaps because it is just a small part of an originally bigger system, and resembles normal thrust stacks rather than crustal ramps.

6. Conclusions

The data are inferred to indicate different provenances of the Dyrs kard and Kvitenut nappes, which subsequently underwent a common Sveconorwegian evolution including early magmatic activity (999 – 985 Ma), metamorphism and thrusting, corresponding to the final

stages of the main Agder phase of the Sveconorwegian orogeny. Late metamorphic titanite growth at 924 Ma during the extensional Dalane phase, presumably reflects reactivation of structures and fluid activity related to magmatism and metamorphism at depth. Whereas the > 1600 Ma protolith age and the remnants of Sveconorwegian granulite facies metamorphism suggests a correlation of the Kvitenut Nappe with what we define as the Gothian terrane, the 1508 Ma volcanic sequence in the Dyrskard Nappe has a clear affinity with the Telemarkia terrane. Various lines of evidence lead to the suggestion that overthrusting of the Kvitenut Nappe on top of the Dyrskard Nappe occurred at around 1000 Ma. The distinction between these two nappes suggests that the thrust corresponds to the original boundary between the Western Gneiss Region and Telemarkia, a boundary which is otherwise hidden below the allochthons of the Faltungsgraben and is not exposed in western parts of the Sveconorwegian orogen. The 1500 Ma inherited zircons in the Stavsnuten granite of the Kvitenut Nappe suggests that the granite was generated in a Telemarkia terrane during convergence. The thrust zone between the Kvitenut and the Dyrskard nappes was not significantly reactivated during Caledonian emplacement of the Hardanger-Ryfylke Nappe Complex and thus the nappes were transported as one block.

References

- Andersen, T.B., 1998. Extensional tectonics in the caledonides of southern Norway, an overview. *Tectonophysics* 285, 333-351 doi:10.1016/s0040-1951(97)00277-1.
- Andersen, T., 2005. Terrane analysis, regional nomenclature and crustal evolution in the Southwest Scandinavian Domain of the Fennoscandian Shield. *GFF* 127, 159-168.
- Andersen, T.B., Andresen, A., 1994. Stratigraphy, tectonostratigraphy and the accretion of outboard terranes in the Caledonides of Sunnhordland, W. Norway. *Tectonophysics* 221, 71-84.
- Andersen, T., Andresen, A., Sylvester, A.G., 2002. Timing of late- to post-tectonic Sveconorwegian granitic magmatism in South Norway. *NGU-Bulletin* 440, 5-18.
- Andersen, T.B., Jamtveit, B., 1990. Uplift of the deep crust during orogenic extensional collapse – a model based on field studies in the Sogn-Sunnfjord region of Western Norway. *Tectonics* 9, 1097-1111.
- Andresen, A., 1972. Petrografiske og strukturegeologiske undersøkelser i fjellstrøket nord for Haukelisæter. Unpublished cand. Real. Thesis, Universitetet i Oslo. 138pp.
- Andresen, A., 1974. Petrography and structural history of the Caledonian rocks north of Haukelisæter, Hardangervidda, NGU-Bulletin 27, 1-52.
- Andresen, A., Gabrielsen, R.H., 1979. Major element chemistry of metavolcanic rocks and tectonic setting of the precambrian Dyrskard Group, Hardangervidda, South-Norway. *Norsk Geologisk Tidsskrift* 59, 47-57.
- Andresen, A., Heier, K.S., Jorde, K., Naterstad, J., 1974. A preliminary Rb/Sr geochronological study of the Hardangervidda-Ryfylke nappe system in the Røldal area, south Norway. *Norsk Geologisk Tidsskrift* 54, 35-47.
- Andresen, A., Færseth, R., 1982. An evolutionary model for the southwest Norwegian Caledonides. *American Journal of Science* 282, 756-782.
- Bingen, B., Andersson, J., Söderlund, U., Möller, C., 2008a. The Mesoproterozoic in the Nordic countries. *Episodes* 31, 29-34.
- Bingen, B., Birkeland, A., Nordgulen, O., Sigmond, E.M.O., 2001. Correlation of supracrustal sequences and origin of terranes in the Sveconorwegian orogen of SW Scandinavia: SIMS data on zircon in clastic metasediments. *Precambrian Res* 108, 293-318 doi:10.1016/s0301-9268(01)00133-4.
- Bingen, B., Nordgulen, O., Viola, G., 2008b. A four-phase model for the Sveconorwegian orogeny, SW Scandinavia. *Norwegian Journal of Geology* 88, 43-72.
- Bingen, B., Skar, O., Marker, M., Sigmond, E.M.O., Nordgulen, O., Ragnhildstveit, J., Mansfeld, J., Tucker, R.D., Liegeois, J.P., 2005. Timing of continental building in the Sveconorwegian orogen, SW Scandinavia. *Norwegian Journal of Geology* 85, 87-116.
- Bingen, B., Solli, A., 2009. Geochronology of magmatism in the Caledonian and Sveconorwegian belts of Baltica: synopsis for detrital zircon provenance studies. *Norwegian Journal of Geology* 89, 267-290.
- Bingen, B., van Breemen, O., 1998. U-Pb monazite ages in amphibolite- to granulite-facies orthogneiss reflect hydrous mineral breakdown reactions: Sveconorwegian Province of SW Norway. *Contrib Mineral Petrol* 132, 336-353 doi:10.1007/s004100050428
- Cherniak, D.J., Watson, E.B., 2001. Pb diffusion in zircon. *Chemical Geology* 172, 5-24.
- Connelly, J.N., 2001. Degree of preservation of igneous zonation in zircon as a signpost for concordancy in U/Pb geochronology. *Chemical Geology* 172, 25-39.

- Corfu, F., Andersen, T.B., 2002. U-Pb ages of the Dalsfjord Complex, SW-Norway, and their bearing on the correlation of allochthonous crystalline segments of the Scandinavian Caledonides. *International Journal of Earth Sciences* 91, 955-963.
- Corfu, F., Heim, M., 2011. U-Pb geochronology of the Southern Scandinavian Caledonides: The Mesoproterozoic Espedalen anorthosite-gabbro-norite massif and associated rocks. *Mineralogical Magazine* 75, 695.
- Corfu, F., Roberts, R.J., Torsvik, T.H., Ashwal, L.D., Ramsay, D.M., 2007. Peri-Gondwanan elements in the Caledonian Nappes of Finnmark, Northern Norway: Implications for the paleogeographic framework of the Scandinavian Caledonides. *American Journal of Science* 307, 434-458 doi:10.2475/02.2007.05.
- Cuthbert, S.J., Carswell, D.A., Krogh-Ravna, E.J., Wain, A., 2000. Eclogites and eclogites in the Western Gneiss Region, Norwegian Caledonides. *Lithos* 52, 165-195 doi:10.1016/s0024-4937(99)00090-0.
- Cuthbert, S.J., Harvey, M.A., Carswell, D.A., 1983. A tectonic model for the metamorphic evolution of the basal-gneiss complex, western South-Norway. *Journal of Metamorphic Geology* 1, 63-90 doi:10.1111/j.1525-1314.1983.tb00265.x.
- Dahlgren, S., Heaman, L., Krogh, T.E., 1990. Geological evolution and U-Pb geochronology of the Proterozoic Central Telemark area, Norway. *Geonytt* 17, 38-39.
- Fossen, H., 1992. The role of extensional tectonics in the Caledonides of South Norway. *Journal of Structural Geology* 14, 1033-1046.
- Fossen, H., 1998. Timing and kinematics of Caledonian thrusting and extensional collapse, southern Norway: Evidence from Ar-40/Ar-39 thermochronology. *Journal of Structural Geology* 20, 765-781.
- Fossen, H., 2000. Extensional tectonics in the Caledonides: Synorogenic or postorogenic? *Tectonics* 19, 213-224.
- Gaal, G., Gorbatshev, R., 1987. An outline of the Precambrian evolution of the Baltic Shield. *Precambrian Research* 35, 15-52 doi:10.1016/0301-9268(87)90044-1.
- Gabrielsen, R.H., 1976. En petrografisk og strukturgeologisk beskrivelse av området Stavsnuten, Haukelifjell. Unpublished cand. Real. Thesis, University of Oslo.
- Gabrielsen, R.H., 1980. The Precambrian Dyrskard Group of the Hardangervidda-Ryfylke Nappe Complex, Haukelisæter-Røldal Area, Southwestern Norway. *Norges geologiske Undersøkelse* 355, 1-20.
- Gabrielsen, R.H., Naterstad, J., Raheim, A., 1979. Rb-Sr study of a possible precambrian thrust zone, Hardangervidda-Ryfylke Nappe Complex, Southwest Norway. *Norsk Geologisk Tidsskrift* 59, 253-263.
- Gee, D.G., Kumpulainen, R., Roberts, D., Stephens, M.B., Thon, A., Zachrisson, E., 1985. Scandinavian Caledonides tectonostratigraphic map. in: Gee DG, Sturt BA (eds) *The Caledonide Orogen-Scandinavia and related areas*. John Wiley & Sons, Chichester, UK, pp. 1266.
- Glodny, J., Kühn, A., Austrheim, H., 2007. Diffusion versus recrystallization processes in Rb-Sr geochronology: Isotopic relics in eclogite facies rocks, Western Gneiss Region, Norway. *Geochimica et Cosmochimica Acta* 72, 2, 506-525.
- Gray, J.W., 1978. Structural history and Rb-Sr geochronology of Eksingedalen, west Norway. University of Aberdeen.
- Griffin, W.L., Brueckner, H.K., 1980. Caledonian Sm-Nd ages and a crustal origin for Norwegian eclogites. *Nature* 285, 319-321 doi:10.1038/285319a0.

- Jaffey, A.H., Flynn, K.F., Glendenin, L.E., Bentley, W.C., Essling, A.M., 1971. Precision measurement of half-lives and specific activities of U-235 and U-238. *Physical Review C* 4, 1889 doi:10.1103/PhysRevC.4.1889.
- Jorde, K., 1973. En petrografisk og strukturgeologisk undersøkelse av parautoktone og alloktone bergarter i området Røldal-Seljestad. Unpublished cand. Real. Thesis, University of Oslo.
- Kildal, E.S., 1973. Meta-andesites in the Caledonides in the Suldal Area, Ryfylke. *Norges geologiske Undersøkelse* 288, 27-51.
- Kirkland, C.L., Daly, J.S., Whitehouse, M.J., 2007. Provenance and terrane evolution of the Kalak Nappe Complex, Norwegian Caledonides: Implications for neoproterozoic paleogeography and tectonics. *Journal of Geology* 115, 21-41 doi:10.1086/509247.
- Kirkland, C.L., Daly, J.S., Whitehouse, M.J., 2008. Basement-cover relationships of the Kalak Nappe Complex, arctic Norwegian Caledonides and constraints on neoproterozoic terrane assembly in the North Atlantic Region. *Precambrian Res* 160, 245-276 doi:10.1016/j.precamres.2007.07.006.
- Krogh, T.E., 1982. Improved accuracy of U-Pb zircon dating by selection of more concordant fractions using a high-gradient magnetic separation technique. *Geochimica et Cosmochimica Acta* 46, 631-635.
- Kullerød, L., Tørudbakken, B.O., Illebekk, S., 1986. A compilation of radiometric age determination from the Western Gneiss Region, South Norway. *NGU-Bulletin* 406, 1742.
- Kylander-Clark, A.R.C., Hacker, B.R., Johnson, C.M., Beard, B.L., Mahlen, N.J., 2009. Slow subduction of a thick ultrahigh-pressure terrane. *Tectonics* 28 doi:10.1029/2007tc002251.
- Laajoki, K., Corfu, F., 2007. Lithostratigraphy of the Mesoproterozoic Vemork formation, central Telemark, Norway. *Bulletin of the geological Society of Finland* 79, 41-67.
- Ludwig, K.R., 2009. Isoplot 4.1. A geochronological toolkit for Microsoft Excel. *Berkeley Geochronology Center Special Publications* 4, 76.
- Lundmark, M., Corfu, F., 2008. Late-orogenic Sveconorwegian massif anorthosite in the Jotun Nappe Complex, SW Norway, and causes of repeated AMCG magmatism along the Baltoscandian margin. *Contributions to Mineralogy and Petrology* 155, 147-163.
- Lundmark, A.M., Corfu, F., Spürger, S., Selbekk, R.S., 2007. Proterozoic evolution and provenance of the high-grade Jotun Nappe Complex, SW Norway: U-Pb geochronology. *Precambrian Research* 159, 133-154 doi:10.1016/j.precamres.2006.12.015.
- Mattinson, J.M., 2005. Zircon U-Pb chemical abrasion ("CA-TIMS") method: Combined annealing and multi-step partial dissolution analysis for improved precision and accuracy of zircon ages. *Chemical Geology* 220, 47-66 doi:10.1016/j.chemgeo.2005.03.011.
- Naterstad, J., Andresen, A., Jorde, K., 1973. Tectonic succession of the Caledonian Nappe Front in the Haukelisæter-Røldal Area, Southwest Norway. *Norges geologiske Undersøkelse* 292, 1-20.
- Ramberg, I.B., Bryhni, I., Nøttvedt, A., Rangnes, K., 2008. The Making of a Land, *Geology of Norway*. Trondheim.
- Roberts, D., 2003. The Scandinavian Caledonides: event chronology, palaeogeographic settings and likely, modern analogues. *Tectonophysics* 365, 283-299 doi:10.1016/s0040-1951(03)00026-x.

- Roffeis, C., Corfu, F., Austrheim, H., 2012. Evidence for a Caledonian amphibolite to eclogite facies pressure gradient in the Middle Allochthon Lindås Nappe, SW-Norway. *Contributions to Mineralogy and Petrology* doi: 10.1007/s00410-012-0727-7.
- Røhr, T.S., Corfu, F., Austrheim, H., Andersen, T.B., 2004. Sveconorwegian U-Pb zircon and monazite ages of granulite-facies rocks, Hisarøya Gulen, Western Gneiss Region, Norway. *Norwegian Journal of Geology* 84, pp. 251-256.
- Schärer, U., 1980. U-Pb and Rb-Sr dating of a polymetamorphic nappe terrain - the Caledonian Jotun Nappe, Southern-Norway. *Earth and Planetary Science Letters* 49, 205-218 doi:10.1016/0012-821x(80)90065-5.
- Schärer, U., Wilmar, E., Duchesne, J.C., 1996. The short duration and anorogenic character of anorthosite magmatism: U-Pb dating of the Rogaland complex, Norway. *Earth and Planetary Science Letters* 139, 335-350.
- Sigmond, E.M., Andresen, A., 1976. A Rb-Sr isochron age on metaandesites from Skorpehei, Suldal, south Norway. *Norsk Geologisk Tidsskrift* 56:315-319
- Skår, A., Furnes, H., Claesson, S., 1994. Proterozoic orogenic magmatism within the Western Gneiss Region, Sunnfjord, Norway. *Norsk Geologisk Tidsskrift* 74, 114-126.
- Skår, O., Pedersen, R.B., 2003. Relations between granitoid magmatism and migmatization: U-Pb geochronological evidence from the Western Gneiss Complex, Norway. *Journal of Geological Society* 160, 935-946 doi:10.1144/0016-764901-121.
- Stacey, J.S., Kramers, J.D., 1975. Approximation of terrestrial lead isotope evolution by a 2-stage model. *Earth and Planetary Science Letters* 26, 207-221.
- Stephens, M.B., Gee, D.G., 1985. A tectonic model for the evolution of the eugeoclinal terranes in the central Scandinavian Caledonides. In: Gee DG, Sturt, B.A. (Eds.) *The Caledonide Orogen: Scandinavia and related Areas*, vol 2. John Wiley, Hoboken, N.J., pp 953-978.
- Stephens, M.B., Wahlgren, C.H., Weijermars, R., Cruden, A.R., 1996. Left-lateral transpressive deformation and its tectonic implications, Sveconorwegian orogen, Baltic shield, southwestern Sweden. *Precambrian Res* 79, 261-279 doi:10.1016/0301-9268(95)00097-6.
- Torske, T., 1982. Structural effects on the Proterozoic Ullensvang Group (West Norway) relatable to forceful emplacement of expanding plutons. *Geologische Rundschau* 71, 104-119.
- Torsvik, T.H., Smethurst, M.A., Meert, J.G., Van der Voo, R., McKerrow, W.S., Brasier, M.D., Sturt, B.A., Walderhaug, H.J. 1996. Continental break-up and collision in the Neoproterozoic and Palaeozoic - A tale of Baltica and Laurentia. *Earth-Science Reviews* 40, 229-258 doi:10.1016/0012-8252(96)00008-6.
- Tucker, R.D., Robinson, P., Solli, A., Gee, D.G., Thorsnes, T., Krogh, T.E., Nordgulen, O., Bickford, M.E., 2004. Thrusting and extension in the scandian hinterland, Norway: New U-Pb ages and tectonostratigraphic evidence. *Am J Sci* 304, 477-532 doi:10.2475/ajs.304.6.477.
- Tucker, R.D., Råheim, A., Krogh, T.E., Corfu, F., 1987. Uranium-lead zircon and titanite ages from the northern portion of the Western Gneiss Region, south-central Norway. *Earth and Planetary Science Letters* 81, 203-211 doi:10.1016/0012-821x(87)90156-7.
- Wennberg, O.P., Milnes, A.G., Winswold, I., 1998. The northern Bergen Arc Shear Zone - an oblique-lateral ramp in the Devonian extensional detachment system of western Norway. *Norwegian Journal of Geology (NGT)* 78, 169-184.

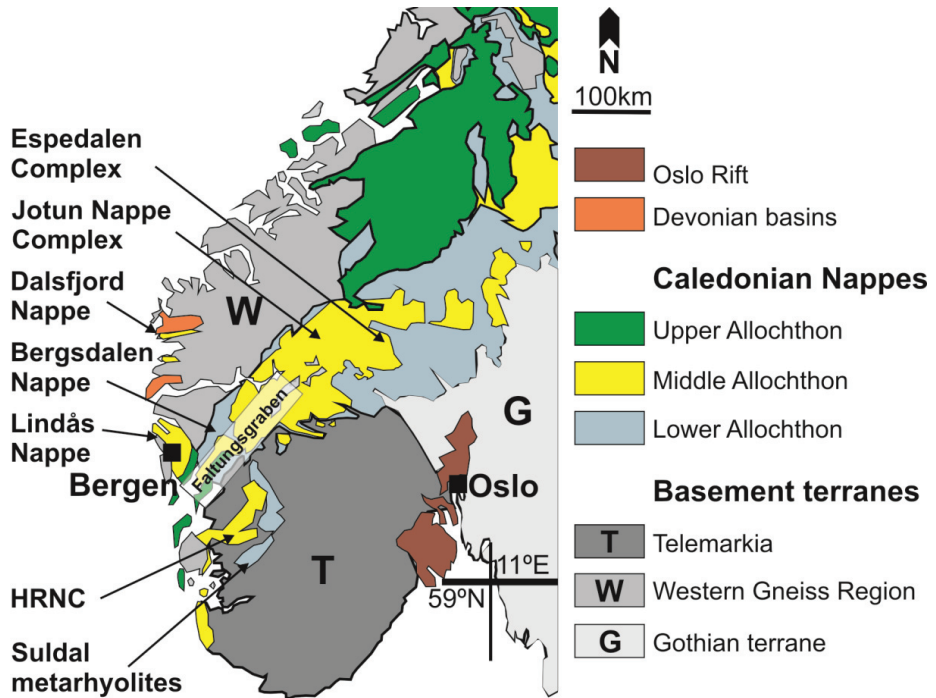


Fig. 1. Tectonostratigraphy of the SW Norwegian Caledonides (after Gee et al., 1985). The study area lies in the Hardanger-Ryfylke Nappe Complex.

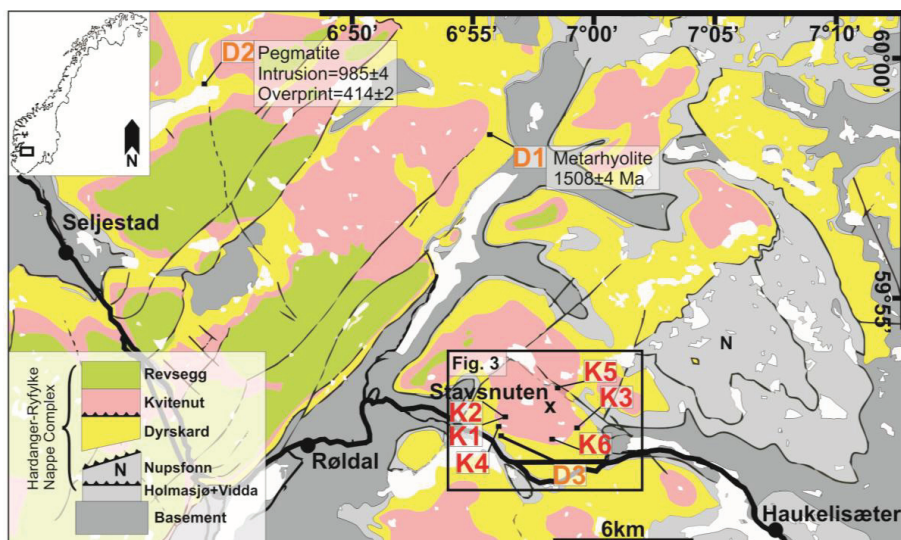


Fig. 2. Geological map of the study area, north of Haukelisæter-Røldal-Seljestad (modified after <http://geo.ngu.no/kart/berggrunn/>). The distribution of the different nappe sheets is shown with color coding, tectonic relations are given within the legend. Sample localities in the Dyrskard Nappe are marked with D, in the Kvitenut Nappe with K. The framed area around Stavsnuten, containing all Kvitenut sample localities, is enlarged and shown in more detail in Fig. 3.

Paper #2, Figure 3

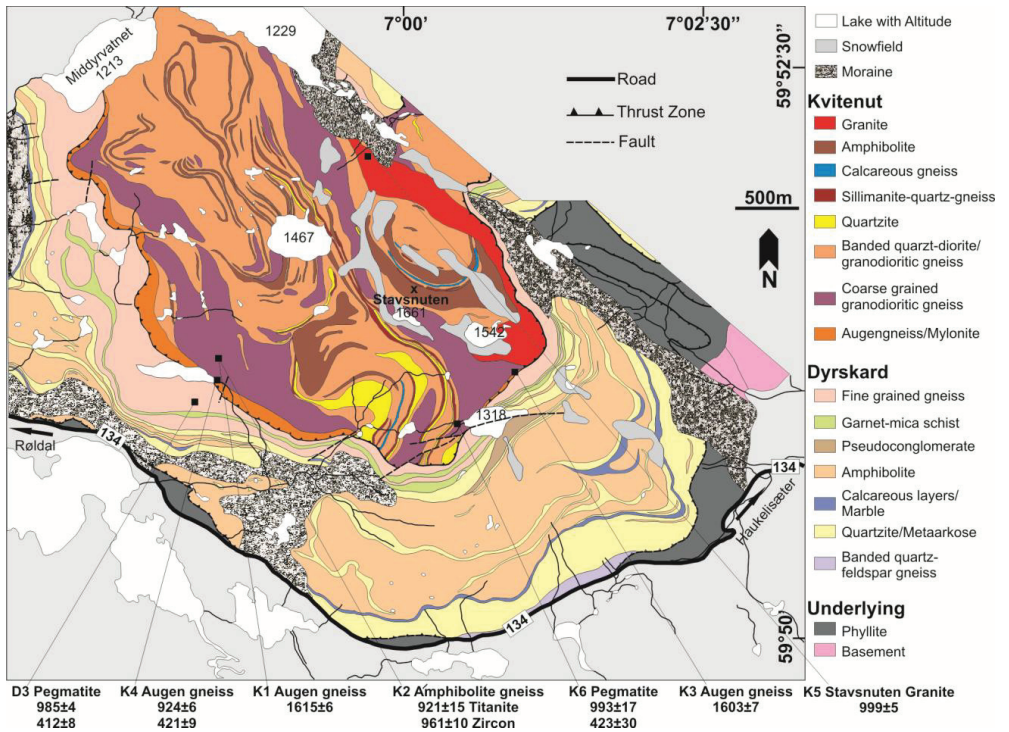


Fig. 3. Geological map of the Stavsnuten area (after Gabrielsen, 1976). Kvitenut rocks overly the Dyrskard nappe. Sample localities (same as in Fig. 2) are marked and given with corresponding ages in Ma. Lakes are given with altitude.

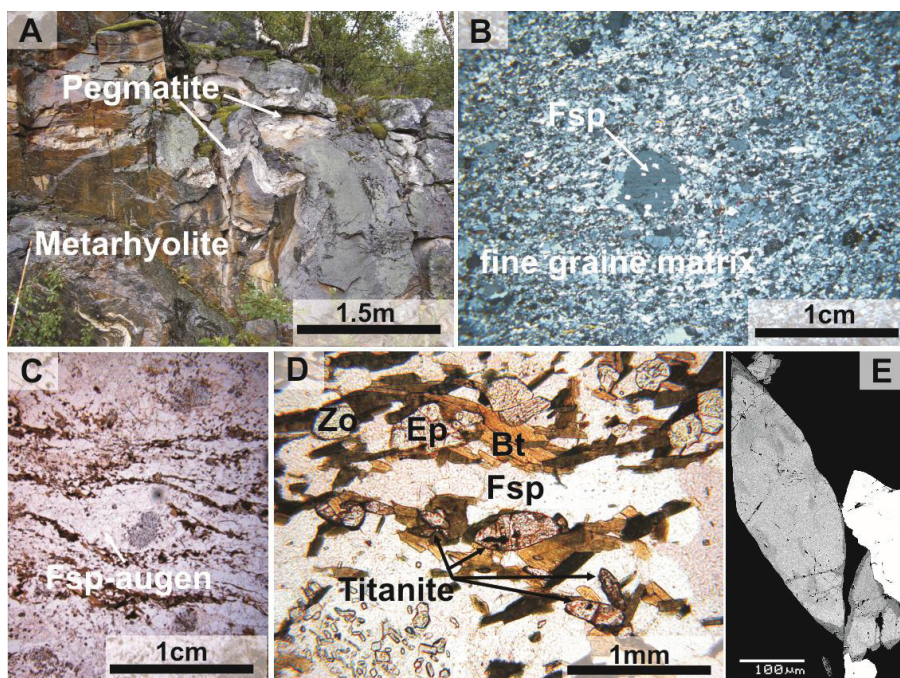


Fig. 4. Samples in the field and in thin section. (A) Metarhyolite outcrop in the Dyrskard Nappe, cut by folded pegmatite (sample D2). (B) Metarhyolite (D1) in thin section. Corroded feldspar phenocrysts occur in a fine grained, quartz rich matrix. (C) Augen gneiss - blastomylonite at the base of Kvitenut (sample K4). Mainly biotite with additional epidote form layers wrapping around feldspar porphyroclasts. (D) Detail of the same sample: large titanite co-genetic with epidote, zoisite and biotite, together delineating the augen-structure. (E) CL-image of a large titanite in the foliation from (D). Only slight re-crystallization is observed at the tips of the grain.

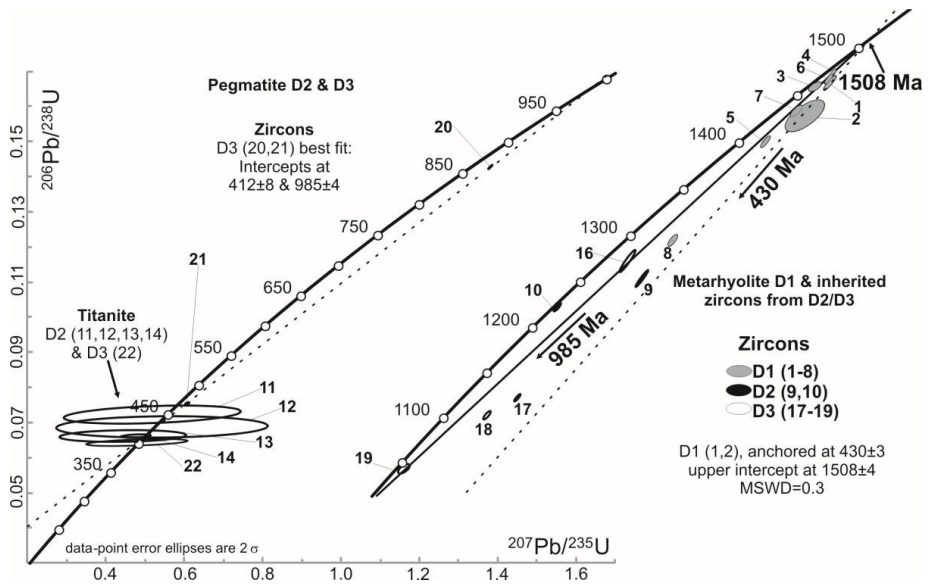


Fig. 5. Analytical data for Dyrskard rocks. Sample names are the same as in Fig. 2, the numbering of the data points is congruent with Table 1. Uncertainty ellipses represent 2σ.

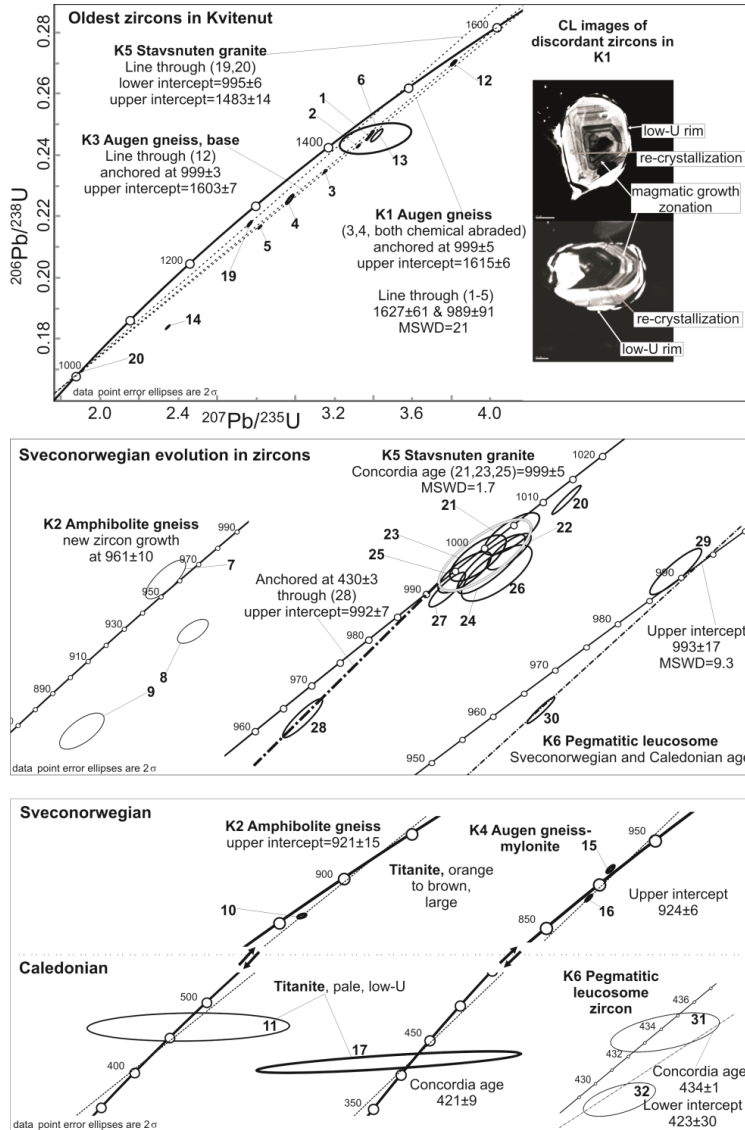


Fig. 6. Analytical data for Kvitenut rocks. The sample names are as in Figs. 2 and 3, the numbering of the data points is congruent with Table 1. Uncertainty ellipses represent 2 σ .

Paper #2, Figure 7

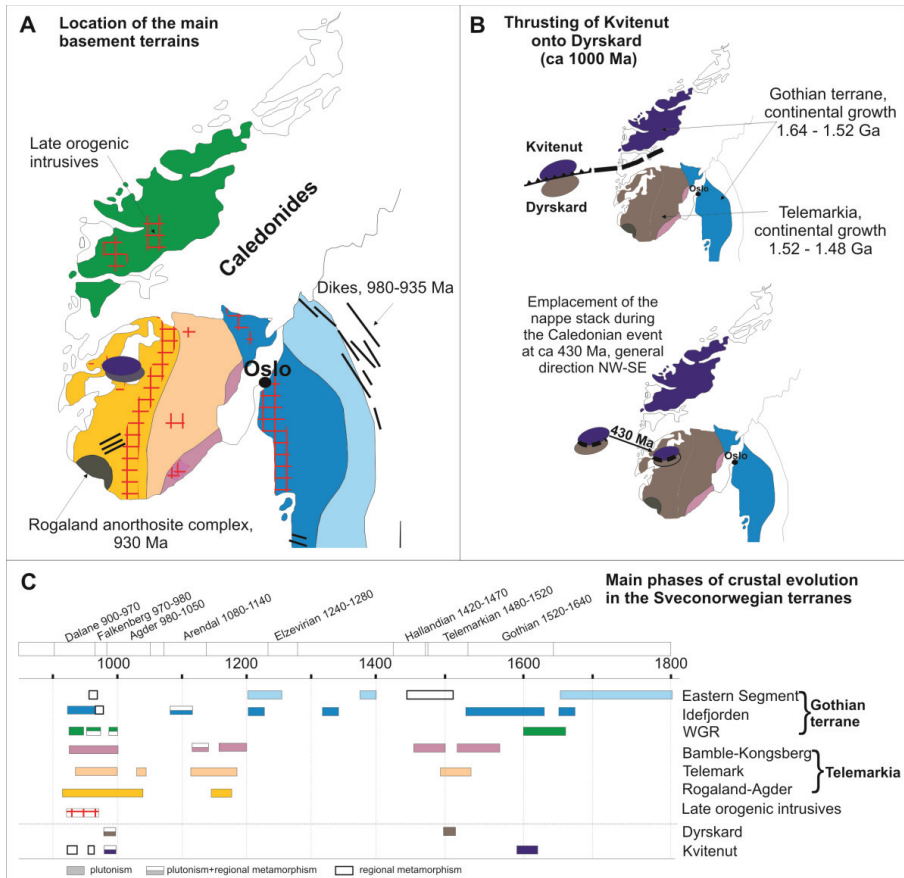


Fig. 7. (A) Basement terranes in SW-Norway. The terranes are given with a summary of ages, adapted from Bingen et al. (2005). (B) The assumed provenance of the Kvitenut and Dyrs kard nappes, shown as ellipses in the western continuation of Baltica. The thrusting of the Kvitenut Nappe onto the Dyrs kard Nappe occurred at ca 1000 Ma, and we infer that the thrust zone represents the border between the Gothian terrane and Telemarkia. The NW-SE transport of the coupled nappe stack during the Caledonian event is shown in the lower sketch. (C) A comparison of intrusive and metamorphic ages, from crustal formation to the Sveconorwegian event, for the basement terranes in SW Norway, and for the Kvitenut and Dyrs kard nappes. The color coding follows (A).

Appendix to Paper #2: Table

Table 1 Zircon and titanite U-Pb data, Hardanger-Ryfylke Nappe Complex

No.	Properties	Weight [μg]	Pbt [ppm]	U [ppm]	Th/U	Pbcom [ppm]	Pbcom [pg]	206/204	207/235	2 sigma [abs]	206/238	2 sigma [abs]	rho	207/206	2 sigma [abs]	206/238	[Ma]	[Ma]
(a)																		
Dysrard - D1 Metarhyolithe, 59°57'57.66"N 6°56'44.4"E																		
1	idiomorph	1	80	308	0.31	0.00	0.6	8392	3.284	0.016	0.25472	0.00115	0.94	0.09351	0.00016	1462.8	1477.3	1498.3
2	tip, clear, CA	1	45	180	0.31	0.00	1.2	2283	3.196	0.054	0.24807	0.00251	0.71	0.09343	0.00112	1428.5	1456.1	1486.5
3	2gr. equant, clear	19	3	10	0.33	0.02	2.4	1311	3.231	0.015	0.25407	0.00075	0.69	0.09225	0.00032	1459.4	1464.7	1472.4
4	2gr. equant, incl	21	15	57	0.33	0.05	3.1	6176	3.291	0.009	0.25672	0.00060	0.92	0.09297	0.00011	1473.0	1478.8	1487.2
5	piece, middle part of prism, CA	1	68	267	0.43	0.00	0.6	6538	3.061	0.013	0.24274	0.00083	0.91	0.09145	0.00016	1400.9	1422.9	1456.0
6	prism, brownish in the middle	3	31	120	0.31	0.00	0.8	7471	3.281	0.013	0.25571	0.00085	0.93	0.09307	0.00014	1467.8	1476.6	1489.2
7	prism, 1 black incl	3	8	31	0.31	0.00	1.0	1536	3.168	0.016	0.24911	0.00087	0.82	0.09222	0.00027	1433.9	1449.3	1472.0
8	tip, clear, CA	1	42	186	0.35	0.00	0.8	3104	2.743	0.013	0.22251	0.00084	0.82	0.08942	0.00025	1295.1	1340.3	1413.1
Dysrard - D2 Pegmatite in metarhyolite, 59°58'8.76"N 6°43'7.74"E																		
9	tip, [101] pyramid	1	99	409	0.79	0.00	0.6	9231	2.64	0.02	0.2147	0.0014	0.96	0.08908	0.00016	1253.7	1310.9	1405.9
10	tip	1	26	119	0.49	0.00	0.7	2401	2.35	0.01	0.20867	0.00070	0.84	0.08151	0.00020	1221.8	1226.1	1233.8
11	tit*, 3gr. pieces, clear	1	9	16	0.03	0.71	9.5	27	0.52	0.19	0.0722	0.0020	0.35	0.052	0.018	449.6	424.2	288.7
12	tit*, pale	38	2	3	0.82	1.92	75.8	25	0.54	0.22	0.0687	0.0024	0.09	0.057	0.023	428.6	440.4	502.5
13	tit*, 1gr. clear, >200 μm, equant	8	4	8	0.34	3.28	28.1	28	0.44	0.13	0.0662	0.0014	0.16	0.048	0.014	413.5	372.4	123.7
14	tit*, 2gr. octahedral, clear, <100 μm	1	12	86	0.09	6.55	8.5	61	0.48	0.03	0.06614	0.00042	0.40	0.0523	0.0034	412.8	395.9	297.9
15	tit, 1gr. octahedral, partly milky	7	4	6	3.35	26.0	26.5	used for Pb correction, $^{206}\text{Pb}/^{238}\text{U} = 19.221 \pm 0.2$, $^{207}\text{Pb}/^{235}\text{U} = 15.697 \pm 0.129$										
Dysrard - D3 Concordant pegmatite vein in fine-grained schistose gneiss, 59°51'2.34"N 006°58'32.94"E																		
16	short prism, sub. clear	1	58	260	0.34	0.00	1.3	2839	2.588	0.023	0.21825	0.00183	0.95	0.08600	0.00024	1272.6	1297.2	1338.1
17	short prism	1	98	511	0.32	0.25	2.3	2687	2.208	0.009	0.19021	0.00063	0.89	0.08418	0.00016	1122.5	1183.5	1296.8
18	3 pieces, rim from 19, partly brownish	1	40	217	0.27	0.00	0.7	3698	2.104	0.010	0.19658	0.00069	0.82	0.08180	0.00023	1102.8	1150.2	1240.6
19	round clear core, rim is 18	1	23	135	0.10	0.02	2.0	751	1.820	0.015	0.17560	0.00075	0.63	0.07515	0.00049	1042.9	1052.5	1072.6
20	piece of prism, partly brownish	3	59	441	0.06	0.00	0.8	15627	1.3814	0.0049	0.14274	0.00046	0.95	0.07019	0.00008	860.1	881.0	933.8
21	200 μm, short prism, metamict	1	304	3911	0.19	22.19	25.7	734	0.6079	0.0039	0.07536	0.00029	0.67	0.05850	0.00028	468.4	482.2	548.5
22	tit*, 3gr., clear, colorless	6	17	26	15.91	97.7	24.2	0.48	used for Pb correction, $^{206}\text{Pb}/^{238}\text{U} = 17.869 \pm 0.05$, $^{207}\text{Pb}/^{235}\text{U} = 15.562 \pm 0.055$									
23	tit, 6gr. white, clear, cauliflower	1	150	0.29	146.77	153.4	17.9											
Kvitnut - K1 Augen gneiss, 59°51'17.82"N 006°58'58.74"E																		
1	clear, round	1	201	750	0.59	0.00	1.2	9971	3.187	0.017	0.24637	0.00125	0.99	0.09381	0.00008	1419.7	1453.9	1504.3
2	long prism, incl	26	44	170	0.55	0.02	2.6	26009	3.1265	0.0075	0.24289	0.00051	0.96	0.09336	0.00006	1401.7	1439.2	1495.1
3	prism, small incl, CA	7	57	232	0.46	0.00	1.8	13049	2.9534	0.0068	0.23468	0.00047	0.95	0.09127	0.00007	1395.7	1452.3	1495.3
4	clear, round, CA	3	75	317	0.46	0.28	2.9	4646	2.775	0.017	0.2255	0.0014	0.90	0.08926	0.00024	1310.8	1348.8	1409.7
5	prism, small incl	6	90	398	0.43	0.09	2.6	12579	2.6203	0.0060	0.21651	0.00043	0.95	0.08777	0.00006	1263.4	1306.3	1377.6
Kvitnut - K2 Amphibolite gneiss, 59°51'17.82"N 006°58'58.74"E																		
6	prism, sub. small incl	1	2	7	0.83	0.00	1.1	120	3.215	0.149	0.24535	0.00407	0.45	0.09504	0.00396	1414.5	1460.8	1528.9
7	prism, sub. small incl	1	13	87	0.03	0.00	1.5	612	1.555	0.022	0.16068	0.00176	0.77	0.07020	0.00064	960.6	952.6	934.1
8	prism, sub. small incl	1	37	215	0.11	5.16	7.5	296	1.592	0.017	0.15495	0.00109	0.64	0.07452	0.00062	928.6	967.1	1055.5
9	prism, sub. small incl	1	10	71	0.07	0.00	1.6	422	1.442	0.025	0.14385	0.00162	0.68	0.07270	0.00092	868.4	906.6	1005.7
10	tit, brown	1	95	587	0.52	6.89	9.3	578	1.351	0.007	0.14230	0.00043	0.56	0.06886	0.00029	857.6	888.0	894.5
11	tit, ca 10gr, pale	72	2	2.7	0.55	1.59	123.6	25.3	0.70	0.24	0.09216	0.00323	0.09	0.05523	0.01851	568.3	539.9	421.6

Kvitenut - K3 Augen gneiss, base, 59°51'19.26"N 7°145.48"E																		
12	short prism, sub, clear	1	150	539	0.36	0.00	1.5	6064	3.616	0.011	0.27005	0.00064	0.85	0.09712	0.00016	1541.1	1553.1	1569.5
13	short prism, sub, clear	1	43	171	0.37	0.00	1.2	2263	3.170	0.024	0.24420	0.00163	0.90	0.09415	0.00032	1408.5	1449.9	1511.1
14	200µm, idiomorph, metamict	10	196	1099	0.23	0.80	10.6	11800	2.1761	0.0081	0.18072	0.00056	0.95	0.08733	0.00011	1070.9	1173.4	1367.8
Kvitenut - K4 Augen gneiss, base, next to lake, 59°51'36.36"N 6°58'51.9"E																		
15	tit, 1gr, orange, clear, rounded	1	266	1640	0.37	10.30	12.6	1269	1.45149	0.00755	0.15293	0.00057	0.81	0.06884	0.00021	917.4	910.5	893.8
16	tit, 1gr, d-orange, no incl	16	65	424	0.37	1.74	30.5	2065	1.40331	0.00579	0.14690	0.00050	0.91	0.06928	0.00012	883.6	890.3	907.2
17	tit*, 5gr, pale, no incl, caulifw	19	2	1.2	0.73	1.58	32.5	20.7	0.45214	0.28018	0.06709	0.00213	0.78	0.04888	0.02910	418.6	378.8	142.0
18	tit, 4gr, pale, clear, prism	13	11	0.6	2.61	10.74	146.0	18.1										
used for Pb correction, $^{206}\text{Pb}_{\text{calc}} = 17.848 \pm 0.049$, $^{207}\text{Pb}_{\text{calc}} = 15.567 \pm 0.054$;																		
Kvitenut - K5 Stavsnuuten granite, 59°52'9.02"N 7°024.84"E																		
19	rounded, clear	1	70	299	0.55	0.00	0.7	6239	2.56972	0.01070	0.21744	0.00077	0.93	0.08571	0.00013	1268.3	1292.1	1331.7
20	brownish, irregular shape, CA	13	571	3500	0.14	0.17	4.4	110959	1.71450	0.00527	0.16971	0.00046	0.96	0.07327	0.00006	1010.5	1014.0	1021.5
21	tip + middle part of long prism	1	21	113	0.64	0.00	0.9	1400	1.68983	0.01030	0.16836	0.00067	0.76	0.07280	0.00029	1003.1	1004.7	1008.3
22	tip, large, CA	2	36	202	0.52	0.11	2.3	1902	1.68868	0.00807	0.16768	0.00059	0.79	0.07304	0.00021	999.3	1004.3	1015.1
23	<100µm, middle part of prism, CA	1	33	179	0.63	0.00	0.4	4230	1.67457	0.01033	0.16740	0.00074	0.74	0.07255	0.00030	997.8	998.9	1001.4
24	rounded, CA	1	40	231	0.43	0.00	1.8	1361	1.68056	0.01248	0.16718	0.00097	0.84	0.07291	0.00030	996.5	1001.2	1011.4
25	tip of short prism, CA	1	34	212	0.15	0.00	1.4	1626	1.66858	0.00982	0.16685	0.00067	0.77	0.07253	0.00028	994.7	996.6	1000.9
26	tip, <100µm, CA	1	15	86	0.54	0.00	0.6	1575	1.68304	0.01306	0.16682	0.00089	0.71	0.07317	0.00040	994.6	1002.1	1018.7
27	tip, clear, CA	1	79	487	0.18	0.00	1.1	4513	1.66074	0.00672	0.16616	0.00055	0.87	0.07249	0.00015	990.9	993.7	999.7
28	long, prism, clear	1	154	971	0.23	0.00	1.0	10300	1.59541	0.00740	0.16109	0.00063	0.90	0.07183	0.00015	962.8	968.4	981.1
Kvitenut - K6 Pegmatitic leucosome, 59°51'1.86"N 7°012.4"E																		
29	tip, clear	1	134	741	0.62	0.00	1.6	4966	1.64891	0.00871	0.16624	0.00074	0.89	0.07194	0.00017	991.3	989.1	984.3
30	2gr, tips, [101]	18	404	2558	0.19	3.57	70.3	6618	1.59363	0.00469	0.16082	0.00042	0.96	0.07187	0.00006	961.3	967.7	982.3
31	2gr, tips, clear	9	7	102	0.47	0.08	2.8	1439	0.53366	0.00407	0.06960	0.00019	0.51	0.05561	0.00037	433.8	434.2	436.8
32	prism, whole grain, incl	4	26	368	0.46	0.41	3.8	1697	0.52948	0.00271	0.06879	0.00017	0.56	0.05583	0.00024	428.8	431.5	445.6

a) main features of analyzed zircons. X00 indicates approximate size of grains in microns. CA = zircon treated with chemical abrasion (Mattinson, 2005), all other zircon fractions air abraded (Krogh1982), prism=prismatic, incl=inclusions, sub=subrounded, all samples are zircon and single grains, unless stated otherwise. Tit=titanite

b) weight and concentrations are known to better than 10%, except for those near and below the ca. 1 µg limit of resolution of the balance.

c) Th/U model ratio inferred from 208/206 ratio and age of sample

d) Pb = total common Pb in sample (initial + blank)

e) raw data, corrected for fractionation and spike

f) corrected for fractionation, spike, blank (206/204=18.3; 207/204=15.555) and initial common Pb (based on Stacey and Kramers, 1975); error calculated by propagating the main sources of uncertainty.

* calculated with measured Pb_{com} values from corresponding sample

Paper #3

*Prepared for Special Publication of the Geological Society, London:
'New perspectives on the Caledonides of Scandinavia and related areas'*

Paper #4

*Prepared for Special Publication of the Geological Society, London:
'New perspectives on the Caledonides of Scandinavia and related areas'*

